



# Combining two complementary micrometeorological methods to measure CH<sub>4</sub> and N<sub>2</sub>O fluxes over pasture

Johannes Laubach<sup>1</sup>, Matti Barthel<sup>1,2</sup>, Anitra Fraser<sup>1</sup>, John E. Hunt<sup>1</sup>, and David W. T. Griffith<sup>3</sup>

<sup>1</sup>Landcare Research, P.O. Box 69040, Lincoln 7640, New Zealand

<sup>2</sup>Department of Environmental Systems Science, ETH Zürich, 8092 Zürich, Switzerland

<sup>3</sup>School of Chemistry, University of Wollongong, Wollongong NSW 2522, Australia

Correspondence to: Johannes Laubach (laubachj@landcareresearch.co.nz)

Received: 29 June 2015 – Published in Biogeosciences Discuss.: 16 September 2015

Revised: 28 January 2016 – Accepted: 13 February 2016 – Published: 2 March 2016

**Abstract.** New Zealand's largest industrial sector is pastoral agriculture, giving rise to a large fraction of the country's emissions of methane (CH<sub>4</sub>) and nitrous oxide (N<sub>2</sub>O). We designed a system to continuously measure CH<sub>4</sub> and N<sub>2</sub>O fluxes at the field scale on two adjacent pastures that differed with respect to management. At the core of this system was a closed-cell Fourier transform infrared (FTIR) spectrometer, which measured the mole fractions of CH<sub>4</sub>, N<sub>2</sub>O and carbon dioxide (CO<sub>2</sub>) at two heights at each site. In parallel, CO<sub>2</sub> fluxes were measured using eddy-covariance instrumentation. We applied two different micrometeorological ratio methods to infer the CH<sub>4</sub> and N<sub>2</sub>O fluxes from their respective mole fractions and the CO<sub>2</sub> fluxes. The first is a variant of the flux-gradient method, where it is assumed that the turbulent diffusivities of CH<sub>4</sub> and N<sub>2</sub>O equal that of CO<sub>2</sub>. This method was reliable when the CO<sub>2</sub> mole-fraction difference between heights was at least 4 times greater than the FTIR's resolution of differences. For the second method, the temporal increases of mole fractions in the stable nocturnal boundary layer, which are correlated for concurrently emitted gases, are used to infer the unknown fluxes of CH<sub>4</sub> and N<sub>2</sub>O from the known flux of CO<sub>2</sub>. This method was sensitive to "contamination" from trace gas sources other than the pasture of interest and therefore required careful filtering. With both methods combined, estimates of mean daily CH<sub>4</sub> and N<sub>2</sub>O fluxes were obtained for 56 % of days at one site and 73 % at the other. Both methods indicated both sites as net sources of CH<sub>4</sub> and N<sub>2</sub>O. Mean emission rates for 1 year at the unfertilised, winter-grazed site were 8.9 (±0.79) nmol CH<sub>4</sub> m<sup>-2</sup> s<sup>-1</sup> and 0.38 (±0.018) nmol N<sub>2</sub>O m<sup>-2</sup> s<sup>-1</sup>. During the same year,

mean emission rates at the irrigated, fertilised and rotationally grazed site were 8.9 (±0.79) nmol CH<sub>4</sub> m<sup>-2</sup> s<sup>-1</sup> and 0.58 (±0.020) nmol N<sub>2</sub>O m<sup>-2</sup> s<sup>-1</sup>. At this site, the N<sub>2</sub>O emissions amounted to 1.21 (±0.15) % of the nitrogen inputs from animal excreta and fertiliser application.

## 1 Introduction

The accurate assessment of greenhouse gas (GHG) fluxes between the biosphere and the atmosphere is crucial to understanding the driving mechanisms of global climate change. While net ecosystem exchange (NEE) of carbon dioxide (CO<sub>2</sub>) fluxes are being measured for multiple years at over 400 sites around the globe, using the eddy-covariance method (Baldocchi, 2014), continuous methane (CH<sub>4</sub>) and nitrous oxide (N<sub>2</sub>O) measurements are still comparably sparse at the ecosystem scale (Nicolini et al., 2013). However, the accounting of full GHG budgets is especially important for agroecosystems as they are the largest global source of N<sub>2</sub>O and CH<sub>4</sub> emissions (Montzka et al., 2011). For instance, Leahy et al. (2004) showed that N<sub>2</sub>O and CH<sub>4</sub> emissions on managed grasslands have the potential to fully counteract the CO<sub>2</sub> sink strength in these ecosystems. This has been confirmed by a European wide synthesis study done at 10 different grasslands sites over 2 years (Soussana et al., 2007). Moreover, among soils from different land-use types, those from grasslands have been shown to have the highest rates of N<sub>2</sub>O emissions, due to high microbial activity stimulated by high soil C (carbon) and N (nitrogen) content (Schaufli et al., 2010).

In order to assess effects of management and land-use changes on net GHG budgets, methods are required to measure GHG fluxes at the scale at which agroecosystems are managed, which is the field scale. Long-term field-scale studies of GHG fluxes in New Zealand's pastoral agroecosystems are so far restricted to CO<sub>2</sub> only (Nieveen et al., 2005; Mudge et al., 2011). Yet, 48 % of the country's total GHG emissions are CH<sub>4</sub> and N<sub>2</sub>O emissions from agriculture (MfE, 2015). We therefore began a project to simultaneously measure the exchange rates of all three GHGs from pastures on a commercial dairy farm. In this paper, we describe and critically assess our methods to measure CH<sub>4</sub> and N<sub>2</sub>O fluxes and report results for these from the first 20 months of this project. The reporting of CO<sub>2</sub> fluxes is kept brief here; for detailed derivation and discussion see Hunt et al. (2016).

Particularly suitable for the field scale are micrometeorological methods (Denmead, 2008). Of these, the eddy-covariance method has steadily increased in popularity since new types of fast and precise gas analysers for CH<sub>4</sub> and N<sub>2</sub>O were shown to be suitable (Eugster et al., 2007; Kroon et al., 2007; Tuzson et al., 2010). In managed grasslands, eddy-covariance measurements with such instruments have since been undertaken, e.g. by Neftel et al. (2010), Merbold et al. (2014), Hörtnagl and Wohlfahrt (2014) and Schrier-Uijl et al. (2014).

Disadvantages of the eddy-covariance method are that the fast analysers for CH<sub>4</sub> and N<sub>2</sub>O are expensive, often specific to a single gas and frequently associated with large measurement errors during periods of small fluxes (Kroon et al., 2010). Therefore, we pursue an alternative approach: we use a slow, closed-cell, multi-gas analyser (Fourier transform infrared (FTIR) spectrometer; see Sect. 2.1 for details), and we combine two other micrometeorological methods in order to maximise the GHG flux information that can be gained from such measurements. One of these methods is a variant of the flux-gradient method (Denmead, 2008), which we shall denote as the gas-gradient ratio (GGR) method. It relies on the equality of turbulent diffusivities for different gas species and is fully described in Sect. 2.3. The other method was first applied by Kelliher et al. (2002) and will here be referred to as the nocturnal storage-ratio (NSR) method. It exploits the fact that during calm nights with stable surface-layer stratification, gases emitted at the surface accumulate over time in the surface layer, much like in a natural "big chamber". For gases originating from the same locations, their mole-fraction increases in the surface layer are strongly correlated, and they are easily detectable (see Sect. 2.4).

Both methods are essentially tracer-ratio methods, where we use CO<sub>2</sub> as the tracer, or reference gas. Therefore, concurrent measurements of CO<sub>2</sub> fluxes are required, for which we employ standard eddy-covariance instrumentation. For calm nights, we follow routine practice to discard measured CO<sub>2</sub> fluxes (considering them unreliable) and replace them with modelled values from a gap-filling algorithm. The suitability

of these modelled tracer fluxes for the NSR method is assessed as part of our data analysis.

Our choice of instruments and methods was largely guided by practical considerations. First, we aimed to undertake a paired-site study on two neighbouring pastures with different managements. Rather than having to acquire and maintain four gas analysers, as required for the eddy-covariance method with two gases at two sites (in addition to the standard CO<sub>2</sub>-flux instrumentation), it appeared a sensible alternative to employ a single multi-gas instrument with a switching system, fed via long air-intake lines. Second, one of the two sites was irrigated by a pivot irrigator that regularly passed over with a clearance height of ca. 2.5 m. This constraint on measurement height made it undesirable to operate bulky open-path analysers. While these conditions were very specific to our experiment, we believe that our combination of methods may be useful and attractive in other measurement situations, too.

It is not intended here to give full greenhouse gas budgets of the dairying operations. That will be the subject of future research, based on longer time series of flux measurements. In particular, this study does not consider CH<sub>4</sub> emissions from grazing animals. We exclude all periods from our analysis during which cattle were present. Following standard practice of dairy farms in New Zealand, these grazing events were of only 1 to 2 days duration each, at an animal density of the order of 100 head ha<sup>-1</sup>. At this density, the fluxes of CH<sub>4</sub> and CO<sub>2</sub> would be dominated by eructation and respiration, respectively, from the cattle. The cattle were then moving point sources in a confined space; to measure accurate and representative fluxes from these would be a challenging task, for which a number of micrometeorological methods have been developed and tested elsewhere (Laubach et al., 2008, 2013; Felber et al., 2015). Instead, we aim to determine exchange rates of the pasture surface itself, which for CH<sub>4</sub> are expected to be at least 2 magnitudes smaller than the emission rates from a grazing cattle herd.

The first objectives of this paper are to describe the GGR method and the NSR method in detail and to identify for each the conditions in which it reliably operates (or otherwise). Based on that assessment, we aim to specify data-filtering criteria for each method. We then compare results between the two methods and assess how they should be combined to obtain reliable annual mean fluxes of CH<sub>4</sub> and N<sub>2</sub>O from the pasture surfaces. In the case of the irrigated pasture, we are able to relate the measured N<sub>2</sub>O fluxes to the N inputs from fertilisation and excreta deposition.

## 2 Materials and methods

### 2.1 Site and farming operations

The study was conducted on an intensively managed dairy farm (ca. 900 cows on 382 ha) on the Canterbury

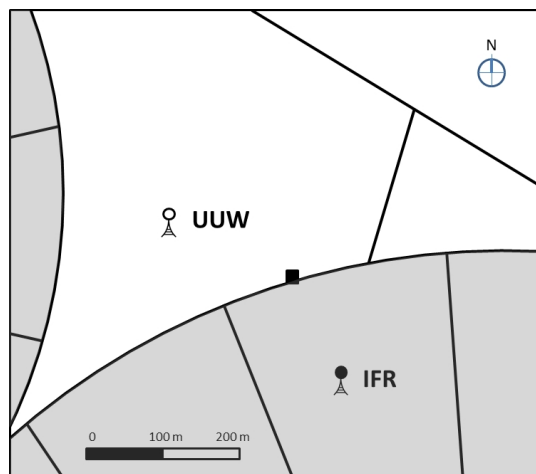


**Figure 1.** Schematic of the experimental area. The shaded areas represent parts of pivot-irrigated intensively managed circles of dairy pasture. The white areas are not irrigated. At each of the labelled locations, UUW (unirrigated, unfertilised, winter-grazed) and IFR (irrigated, fertilised, rotationally grazed), CO<sub>2</sub> fluxes were measured by eddy covariance, and air was sampled from two heights for multi-gas mole-fraction measurements with an FTIR spectrometer. The spectrometer was located in a temperature-controlled hut, indicated with a black square.

Plains, South Island, New Zealand (Lat  $-43^{\circ}35'30.6''$ , Long  $171^{\circ}55'36.6''$ ; 204 m a.s.l.). The soil is a Lismore silty loam, which is moderately stony and well-drained. The farm was converted to irrigated dairying in 2008. The irrigated pasture is dominated by ryegrass (*Lolium perenne* L.) with a minor fraction of white clover (*Trifolium repens* L.). The main irrigated area (263 ha) is circular and subdivided into 19 similarly sized paddocks. Part of the farm is an area of non-irrigated land, wedged between this farm's irrigated circle to the south and a similar irrigated circle of the neighbouring farm to the west (Fig. 1). We established two measurement sites in mid-2012, one inside the irrigated circle at ca. 140 m distance from the perimeter, the other inside the dryland wedge, at a similar distance from its boundaries to south and west. Instrumentation connected to both sites was operated in a hut placed at the boundary between the irrigated and the dryland pasture (Fig. 1).

The farm managers monitored the volumetric water content (VWC) of the pasture soil (10 to 40 cm depth) and used the pivot irrigator to keep the VWC above  $0.2 \text{ m}^3 \text{ m}^{-3}$ . The irrigated pasture was fertilised 9 times annually, on the majority of occasions with urea; in the 2012/13 season, the total application rate was  $18.3 \text{ g N m}^{-2} \text{ yr}^{-1}$ . Throughout the milking season (September to late April) each paddock was grazed 8 to 12 times, usually by 400 to 500 cows. For our measurement site, the times of grazing events were recorded. Effluent collected at the milking shed was recycled to the pasture via irrigator attachments. We will refer to our measurement site on the irrigated, fertilised, rotationally grazed

pasture as the “IFR site”; for future reference in the Fluxnet network it has been named “NZ-BFm” (D. Papale, personal communication, 2016).

The dryland pasture was used for winter-grazing once in July 2012, prior to the start of our measurements, and once in May 2013; otherwise, it was not managed during the 2012/13 season. The measurement site there is labelled as the “UUW site” (unirrigated, unfertilised, winter-grazed); its future Fluxnet name will be “NZ-BFu”. On 28 October 2013 the pasture was sprayed with herbicide, followed by sowing kale (*Brassica oleracea* L., cultivar “corka”) on 20 November, to provide a forage crop for winter 2014.

## 2.2 Instrumentation

### 2.2.1 Mole-fraction measurements of CH<sub>4</sub>, N<sub>2</sub>O and CO<sub>2</sub>

Mole fractions of the trace gases CO<sub>2</sub>, CH<sub>4</sub>, N<sub>2</sub>O and CO were measured simultaneously with a FTIR trace gas analyser built at the University of Wollongong (Griffith et al., 2012). The analyser is equivalent to the now commercially available Spectronus analyser (Ecotech, Knoxfield, VIC, Australia). This instrument performs broadband-spectrum absorption measurements and uses an optimisation algorithm called MALT (multiple atmospheric layer transmission) to retrieve mole fractions of the trace gas species of interest from the measured infrared spectra. For details of both the FTIR hardware and the MALT algorithm see Griffith et al. (2012).

The FTIR was housed in the hut midway between the two measurement sites. From two heights ( $z_1 = 0.76 \text{ m}$ ,  $z_2 = 1.96 \text{ m}$ ), at each site, air was drawn continuously via 170 m long nylon tubing, buried at 0.2 m depth, into 10 L stainless steel cylinders (ballast tanks) inside the hut. A fifth air intake was at 10 m height, next to the hut, to sample gas mole fractions representative of the wider surroundings. All five air streams were drawn in parallel with a dual-head diaphragm pump (2107AC, Gardner Denver Thomas, Sheboygan, Wisconsin, USA). The FTIR was operated in discrete cell-fill mode, sampling air from each of the five ballast tanks once over the course of a 30 min cycle. During every 29th cycle, the measurement from 10 m was skipped, and instead a sample was taken from a cylinder containing air with known mole fractions of the gases of interest (“target tank”), to check for calibration drifts. An external manifold unit with solenoid valves switched between the different sample and calibration intakes. A four-diaphragm oil-free vacuum pump (MV 2 NT, Vacuubrand, Wertheim, Germany) served to evacuate the FTIR's measurement cell to about 2.5 hPa and then to refill it with sample air. Before entering the cell, the sample air was dried in two stages, with a Nafion<sup>®</sup> drier and a magnesium perchlorate trap. This resulted in water vapour mole fractions of  $< 10 \mu\text{mol mol}^{-1}$ , which were included in the mole fractions retrieved by the MALT algorithm.

The FTIR was run in static mode according to the following measurement cycle procedure: (1) cell and manifold evacuation for 120 s, reaching ca. 3 hPa; (2) cell fill to 900 hPa (for up to a maximum duration of 120 s); (3) cell pressure stabilisation for 60 s; and (4) spectrum collection and analysis for 60 s, then wait to the end of 6 min and repetition of these steps for the next intake line. Because the previous sample was not completely removed from the cell, the measured mole fractions were corrected for the residual sample in the cell from the previous measurement. Since [N<sub>2</sub>O] and [CH<sub>4</sub>] differences between intakes were often less than the resolution limits (see Results), we tested whether the measurement precision could be improved by allowing more time for step 4. This was found to be the case, therefore in a new measurement cycle, the time for step 4 was increased sevenfold, allowing far more individual spectra to be collected and analysed for each cell fill. As the new cycle required 60 min total duration for the five intakes, intakes at only one site could be sampled each half-hour. Therefore, the increased precision came at the cost of halving the data yield. With more time per intake available, the cell-fill pressure was increased to 950 hPa (to achieve a further modest gain in precision) and up to 140 s were allowed for the filling process (step 2). The new cycle was used from 15 October 2013 onwards.

The hut temperature was controlled at 20 (±2) °C, and the measurement cell of the FTIR was thermostat-regulated to 30 °C. Cell temperature during measurements was recorded and used in the retrieval of gas mole fractions from the spectra (Griffith et al., 2012). The cell temperature was found to respond to changes in hut temperature at a rate of 0.01 K K<sup>-1</sup>.

The FTIR was calibrated with three different gas cylinders of clean Southern Hemisphere background air, spiked with varying mole fractions for each species of interest. These cylinders had been filled and their contents composition measured by the National Institute of Water and Atmospheric Research (Wellington, New Zealand), following the standards of the WMO's Global Atmospheric Watch programme. Calibrations were carried out 8 times over a 20-month period and yielded very consistent results: the calibration slopes (of measured vs. nominal mole fractions) showed no systematic variation over time, and their relative standard deviations were 0.14 % for CO<sub>2</sub>, 0.08 % for CH<sub>4</sub> and 0.16 % for N<sub>2</sub>O.

## 2.2.2 CO<sub>2</sub>-flux measurements and gap-filling

At each site, an eddy-covariance (EC) system was operated to measure the fluxes of CO<sub>2</sub>, water vapour, heat and momentum at 1.86 m above ground. The system consisted of an enclosed infrared gas analyser to measure CO<sub>2</sub> and H<sub>2</sub>O vapour concentrations (LI-7200, LI-COR Biosciences, Lincoln, NE, USA) and an ultrasonic anemometer to measure the wind vector and temperature (WindMaster Pro, Gill Instruments, Lymington, Hampshire, UK). The raw 20 Hz time series

were collected with an Analyzer Interface Unit (LI-7550, LI-COR Biosciences, Lincoln, NE, USA). Data corrections, averaging and flux computation were performed with the open-source software EddyPro (LI-COR Biosciences, Lincoln, NE, USA). Further details of the EC set-up are given in Hunt et al. (2016).

The CO<sub>2</sub>-flux data were filtered to exclude grazing periods, periods of instationary wind conditions and periods of low turbulence. The last were flagged by  $\sigma_w = 0.12 \text{ m s}^{-1}$ , where  $\sigma_w$  is the standard deviation of vertical wind speed, following Acevedo et al. (2009) who argue this is a more selective filter than the commonly used friction velocity threshold. The ensuing data gaps were filled with an artificial-neural-network method, known as the SOLO (self-organizing linear output) model (Hsu et al., 2002), which has been shown to be accurate on a daily basis (Eamus et al., 2013).

At the IFR site, small-scale CO<sub>2</sub>-flux measurements with four automated respiration chambers (LI-8100A, LI-COR Biosciences, Lincoln, NE, USA) were available for part of the measurement period. These chambers were placed ca. 3 m from the EC mast, within a fenced area from which the cows were excluded. They received the same irrigation and fertilisation applications as the surrounding paddock. The grass inside the chambers was cut manually when the surrounding paddock was grazed, and on these occasions, urea was hand applied to simulate the additional N input from excreta deposited by grazing animals. Data from these chambers are used to corroborate the nocturnal CO<sub>2</sub> fluxes obtained from EC measurements and SOLO gap-filling.

## 2.2.3 Ancillary measurements

Alongside the EC measurements, each site was equipped to record half-hourly averages of precipitation, radiation, wind speed and direction, relative humidity, air temperature, soil heat flux and direct and diffuse radiation. Also, soil temperature and soil VWC were recorded in three separate profiles per site, at depths of 5, 10, 25 and 50 cm. Soil temperature was measured with copper/constantan thermocouples and VWC with time-domain reflectometry probes (SM300, Delta-T Devices, Burwell, Cambridge, UK).

## 2.3 Gas-gradient ratio method

The GGR method is a variant of what is commonly known as the flux-gradient method. In the latter, the flux  $F_\chi$  of a gas species  $\chi$  is computed as the product of the (negative) vertical concentration gradient with a turbulent diffusivity. In practice, the infinitesimal gradient is approximated by finite differences, which gives

$$F_\chi = -K_\chi C_{\text{air}} \frac{[\chi]_1 - [\chi]_2}{z_1 - z_2}, \quad (1)$$

where  $[\chi]$  is the mole fraction and  $K_\chi$  the turbulent diffusivity of  $\chi$ ,  $C_{\text{air}}$  the molar density of dry air,  $z$  height

above ground and the subscripts 1 and 2 indicate measurement heights. Upward fluxes (away from the surface) are represented with positive values, following the micrometeorological convention. The diffusivity is parameterised using similarity theory (Oke, 1987; Denmead, 2008). Often, the parameterisation is based on momentum exchange; this approach is also known as the aerodynamic method (Oke, 1987; Denmead, 2008). There, the diffusivity of momentum,  $K_m$ , is usually specified as

$$K_m = k u_* z \phi^{-1}, \quad (2)$$

where  $k$  is the von Kármán constant,  $u_*$  friction velocity, and  $\phi$  a function of stratification. To make use of Eq. (2), the ratio of the diffusivities for momentum and mass,  $K_m/K_\chi$  (named the turbulent Schmidt number) must be known; yet, how this number varies with height scale and flow statistics in the surface layer is difficult to measure and different approaches have yielded contradictory results (Wilson, 2013). By contrast, there is less ambiguity about the relationships between the diffusivities of different scalar variables, such as heat, moisture and trace gas concentrations. For a pair of scalars with similar spatial distribution of their source/sink locations, the diffusivities are equal, except for small differences between heat and gases with regard to effects of thermal stratification. Thus, by measuring the flux and the gradient of a reference scalar variable, the diffusivity can be obtained. For example, Phillips et al. (2007) used heat as the reference variable to derive N<sub>2</sub>O fluxes over pasture, and Griffith et al. (2002) used water vapour as the reference to obtain fluxes of CO<sub>2</sub>, CH<sub>4</sub> and N<sub>2</sub>O. In both cases, this method was largely restricted to daytime (because fluxes and gradients of heat and water vapour are small at night). Here, we use CO<sub>2</sub> as the reference variable, a choice successfully employed to measure CH<sub>4</sub> emissions from rice crops (Miyata et al., 2000; McMillan et al., 2007). From Eq. (1), its turbulent diffusivity is given by

$$K_{\text{CO}_2} = -\frac{F_{\text{CO}_2}}{C_{\text{air}} \Delta[\text{CO}_2]} \Delta z, \quad (3)$$

where  $\Delta$  indicates the difference between heights, i.e.  $\Delta[\text{CO}_2] = [\text{CO}_2]_1 - [\text{CO}_2]_2$  and  $\Delta z = z_1 - z_2$ . Assuming  $K_\chi = K_{\text{CO}_2}$  where  $\chi$  now refers to the non-CO<sub>2</sub> gas species, and inserting Eq. (3) back into Eq. (1) results in

$$F_\chi = \frac{\Delta[\chi]}{\Delta[\text{CO}_2]} F_{\text{CO}_2}. \quad (4)$$

The gas-gradient ratio,  $\Delta[\chi]/\Delta[\text{CO}_2]$ , is independent of flow properties, such as wind speed or stratification.

Since fluxes and gradients of CO<sub>2</sub> undergo sign changes in the morning and evening, periods including these transitions will need to be excluded. It is expected that these periods of near-zero [CO<sub>2</sub>] gradients often coincide with periods that are unsuitable for the GGR method anyway, because the surface-layer undergoes transitions between unstable and

stable stratification and flow conditions will not be steady enough to define a meaningful diffusivity.

## 2.4 Nocturnal storage-ratio method

During clear night-time periods, cooling of the ground surface due to long-wave radiation losses causes stable stratification of the atmospheric surface layer. In this nocturnal inversion layer, turbulent exchange is suppressed and wind speeds are low. Consequently, trace gases emitted from the ground, or the biosphere near the ground, accumulate in this layer over time. This accumulation process underlies the principle of the NSR method. Provided that the spatial distribution and temporal pattern of emissions are similar for different gas species, their mole-fraction increases over time must be strongly correlated with each other. This is illustrated in Fig. 2, where changes in [CH<sub>4</sub>], [CO<sub>2</sub>] and [N<sub>2</sub>O] track each other well: the mole fractions increase sharply when  $\sigma_w$  falls below 0.12 m s<sup>-1</sup>, and they return towards their baseline values when  $\sigma_w$  rises persistently above 0.12 m s<sup>-1</sup>. The correlations between the mole fractions of the trace gases are exploited to link the unknown flux of a gas species  $\chi$  with the known flux of another gas, here CO<sub>2</sub>, as follows (Kelliher et al., 2002; Pendall et al., 2010). The relationship between the mole-fraction increases,  $d[\chi]$  and  $d[\text{CO}_2]$ , is assumed linear and expressed by the slope of a linear regression. The flux of  $\chi$  is then computed as the product of the CO<sub>2</sub> flux with the regression slope:

$$\overline{F_\chi} = \frac{\overline{d[\chi]}}{\overline{d[\text{CO}_2]}} \overline{F_{\text{CO}_2}}, \quad (5)$$

where the overbars indicate whole-night averages. This method is only applied for sufficiently calm nights, and the regression slope is determined separately for each of these.

During calm conditions, flux measurements by eddy covariance are notoriously unreliable. Kelliher et al. (2002) and Pendall et al. (2010) used respiration chambers to measure the CO<sub>2</sub> flux instead. Here, we try a different approach. We define calm conditions by the same low-turbulence threshold that is used to filter the CO<sub>2</sub> fluxes measured by eddy covariance prior to gap-filling, as illustrated in Fig. 2. We then use the CO<sub>2</sub> fluxes constructed by the gap-filling algorithm as inputs for the NSR method. Since Eq. (2) applies to whole nights, it is not the accuracy of the half-hourly gap-filled fluxes that matters, but only the accuracy of their whole-night average. We will assess the suitability of gap-filled CO<sub>2</sub> fluxes for deriving other trace gas fluxes with the NSR method (Sect. 3.3.2).

## 2.5 Measurement period

We analyse measurements from the period 17 August 2012 to 31 March 2014, including one full grazing/irrigation season, the larger fraction of a second season, and the winter between these. The FTIR operated continuously, except for

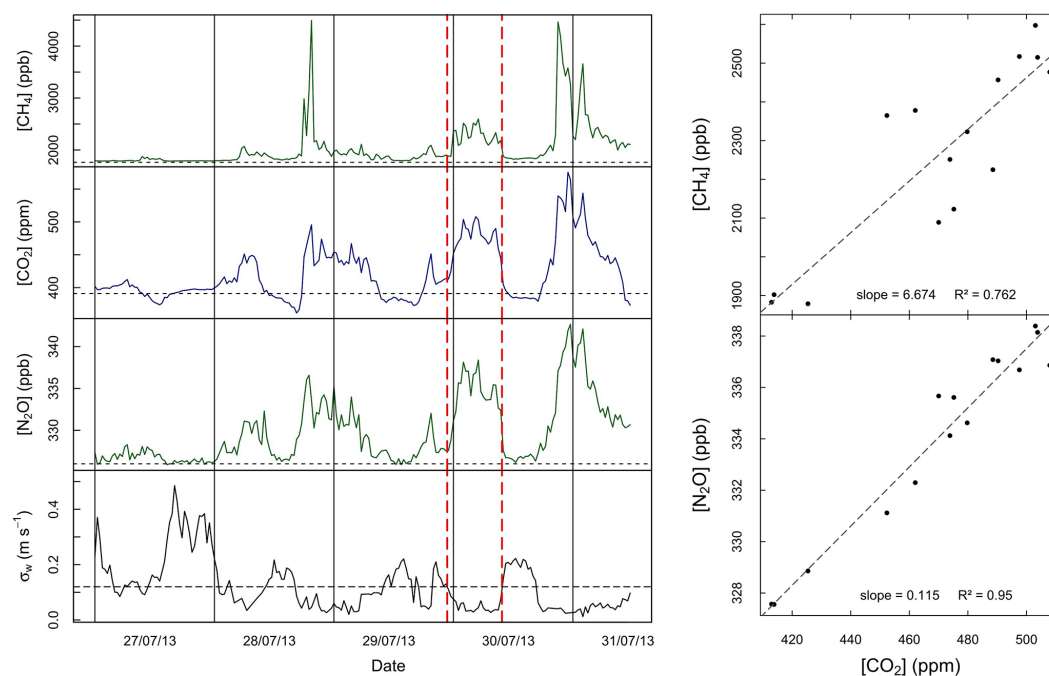


**Figure 2.** Left: evolution of CH<sub>4</sub>, CO<sub>2</sub> and N<sub>2</sub>O mole fractions (from top to bottom) at 0.76 m height, as well as standard deviation of vertical wind speed ( $\sigma_w$ ), at the IFR site, for a few days. Horizontal short-dashed lines indicate the Southern Hemisphere background values of the mole fractions. The horizontal long-dashed line marks the low-turbulence threshold for  $\sigma_w$ . Vertical dashed lines enclose an example period of low turbulence. Right: linear regressions of mole fractions for CH<sub>4</sub> (top panel) and N<sub>2</sub>O (bottom panel) vs. that of CO<sub>2</sub>, for this example period.

short maintenance and calibration periods (a few hours each) and one fortnight of mains-power outage (10 to 24 September 2013) following widespread windstorm damage in the region. Data collected during grazing events were excluded because the CO<sub>2</sub> and CH<sub>4</sub> gradients were dominated by emissions from the animals, which vary erratically with animal positions, and fluxes originating at the pasture surface cannot be retrieved. At the IFR site, grazing events usually lasted only 1 to 2 days; at the U UW site, there were only two grazing periods, in May 2013 and in late October 2013 (just prior to the conversion to kale). The grazing dates of other irrigated paddocks, outside the one containing our measurement site, were not recorded. Data filtering criteria for the GGR method and NSR method are explored in the Results.

### 3 Results

#### 3.1 Soil and vegetation conditions, and CO<sub>2</sub> fluxes

Soil temperatures at 5 cm depth ranged from 2.5 to 22.3 °C at the IFR site and from 1.5 to 23.5 °C at the U UW site, with the minima occurring in early July and the maxima in late January. Rainfall in the year starting 17 August 2012 was 1014 mm, of which 407 mm fell in the warmer half (October–March). At the IFR site, this was supplemented with 425 mm of irrigation to keep the pasture well-watered throughout the

grazing season. The irrigator rotated continuously from mid-spring (October) to mid-autumn (early April), with a return period of about 3 days, applying about 10 L m<sup>-2</sup>. As a result, soil VWC at 5 cm depth stayed above 0.24 m<sup>3</sup> m<sup>-3</sup>. Meanwhile, the U UW site experienced drought conditions from mid-December 2012 to mid-March 2013, with VWC in the range 0.06 to 0.15 m<sup>3</sup> m<sup>-3</sup>.

Over the remaining 7.5 months (after 16 August 2013), 598 mm of natural precipitation occurred. In this period, the start of the irrigation was delayed until mid-November 2013, due to storm damage to the irrigator. When irrigation began, the VWC at 5 cm had already fallen to ca. 0.15 m<sup>3</sup> m<sup>-3</sup>, at both sites. This irrigation season was terminated on 19 February 2014 with the onset of sufficient natural rainfall; the total irrigation in 2013/14 amounted to 345 mm.

Figure 3 shows the time courses of daily mean CO<sub>2</sub> fluxes (net ecosystem exchange), computed from gap-filled half-hourly fluxes, excluding days on which grazing occurred. At the IFR site, each grazing event turned the pasture abruptly from a CO<sub>2</sub> sink (negative mean flux) to a CO<sub>2</sub> source (positive mean flux), while the leaf area index was reduced from 2.7 to 0.6 m<sup>2</sup> m<sup>-2</sup> (Hunt et al., 2016). After a few days of regrowth, the flux reversed sign and the CO<sub>2</sub> sink strength increased steadily, until the next grazing. As a consequence of the regular fertilisation and irrigation, the pasture was highly productive.



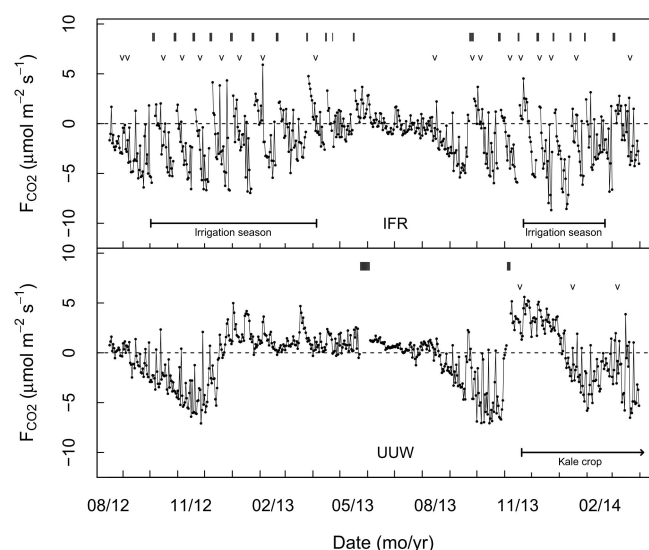


**Figure 3.** Time series of the daily mean CO<sub>2</sub> flux (net ecosystem exchange) at the IFR site (top) and the UUV site (bottom). Grazing times are indicated by bars near the top of each panel. The times of fertiliser applications are marked by “v” symbols.

The UUV site, by contrast, acted as a CO<sub>2</sub> sink mainly in the two spring seasons (September to November) and during the growth of the kale crop in the 2013/14 summer. A prominent feature in Fig. 3 is the change from sink to source in December 2012 as a consequence of the drought conditions. From then until the next spring, the UUV pasture remained a weak CO<sub>2</sub> source. Also clearly visible in Fig. 3 is the disturbance effect of the conversion to kale, making the site temporarily a stronger CO<sub>2</sub> source in November–December 2013, until the kale crop had established itself.

## 3.2 GGR method

### 3.2.1 Mole-fraction gradients and instrument precision

The short-term repeatability of the FTIR’s mole-fraction measurements was determined by repeatedly filling the cell with target-tank air and otherwise following the same switching-cycle sequence as described in Sect. 2.2.1. With the original cycle (total time of 6 min per intake), the standard deviation (SD) of the target-tank [N<sub>2</sub>O] was 0.28 ppb; with the modified cycle (12 min per intake), this was halved to 0.14 ppb (Table 1). For [CH<sub>4</sub>], the SD of the same target-tank samples was 0.58 ppb with the original cycle and reduced to 0.20 ppb with the modified cycle. For [CO<sub>2</sub>], the effect of the change in cycle was less pronounced, with an SD of 0.15 ppm with the original cycle and 0.12 ppm with the modified cycle.

In Table 1, the mean mole fractions using the original cycle and the modified cycle tend to differ by more than the observed SD values (particularly strongly for CH<sub>4</sub>). The likely cause of this is that with the original cycle the spectral mea-

**Table 1.** Results of repeated mole-fraction measurements, with the FTIR spectrometer, of air from a gas cylinder with near-ambient composition (quality control). The two switching cycles are described in Sect. 2.2.1. Numbers in parentheses are standard deviations, from  $n$  successive cell fills.

Switching cycle	$n$	[N <sub>2</sub> O] (ppb)	[CH <sub>4</sub> ] (ppb)	[CO <sub>2</sub> ] (ppm)
Original – 6 min	38	384.07 (0.28)	1805.22 (0.58)	389.53 (0.15)
Modified – 12 min	43	384.53 (0.14)	1808.04 (0.20)	389.79 (0.12)

surements were made before the cell contents had thermally equilibrated. While this lack of equilibrium causes small biases in the mole fractions, the repeatability of these is not affected (as attested by the observed SD values), and mole-fraction differences between intakes (GGR method) or between successive night-time hours (NSR method) are unbiased.

To define a “precision”, the acceptable probability of a single measurement deviating randomly by more than this precision from the mean value must be specified. If we take the acceptable probability as 5 %, then the precision is given as 3 times the SD of repeated sampling. The resolution of a gradient measurement (mole-fraction difference between two intakes) follows directly as  $2^{1/2}$  times that precision: differences smaller than that cannot be considered significantly different from zero. Such non-resolvable mole-fraction differences between intakes occurred frequently, for all three gases. According to Eq. (3), a non-resolvable gradient of gas species  $\chi$  (N<sub>2</sub>O or CH<sub>4</sub>) simply implies a non-resolvable flux of that species, in proportion. When many repeated measurements are made over time to determine a mean flux, those runs with non-resolvable fluxes still make valid contributions: as the standard error of the mean (SEM) decreases with increasing number of samples, the sign (and magnitude) of the mean flux becomes better resolved. Hence, small gradients of [N<sub>2</sub>O] or [CH<sub>4</sub>] were not removed from the data set.

By contrast,  $\Delta[\text{CO}_2]$  appears in the denominator of Eq. (3), with the consequence that small values of it lead to highly uncertain fluxes of  $\chi$ . Thus, the data must be filtered for a minimum  $\Delta[\text{CO}_2]$ . We test this by its effect on the diffusivity, as follows.

### 3.2.2 Turbulent diffusivities

Half-hourly values for the gas diffusivity,  $K_{\text{CO}_2}$ , computed with Eq. (3), are compared in Fig. 4 against the momentum diffusivity,  $K_m$ , for neutral stratification, i.e. using Eq. (2) with  $\phi = 1$ . These data are shown both for all available runs and for two selections with a minimum  $\Delta[\text{CO}_2]$ , of 0.6 and 2.4 ppm (ca. 1 and 4 times the resolution of the FTIR for CO<sub>2</sub>). The unfiltered gas diffusivity data are widely scattered, even outside the margins of the figure. The smaller  $\Delta[\text{CO}_2]$  threshold constrains the  $K_{\text{CO}_2}$  values, by and large, to the range  $-0.6$  to  $1 \text{ m}^2 \text{ s}^{-1}$ , proving that a large part of

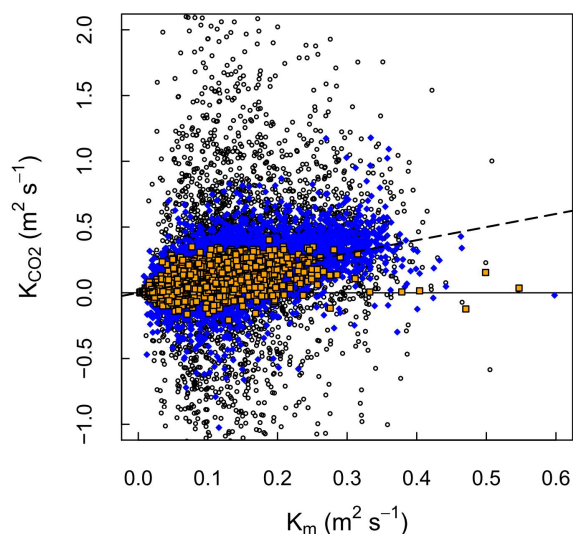


**Figure 4.** Half-hourly values of the turbulent diffusivity of CO<sub>2</sub> (from gradient measurements with the FTIR and flux measurements by eddy covariance) vs. the diffusivity of momentum for neutral stratification (from sonic anemometer data), for the IFR site. Open circles: no filtering of  $\Delta[\text{CO}_2]$  (mole-fraction difference between intake heights), solid diamonds:  $\Delta[\text{CO}_2] < 0.6$  ppm excluded, framed squares:  $\Delta[\text{CO}_2] < 2.4$  ppm excluded. The dashed line is the 1 : 1 line.

the scatter originates from small values in the denominator of Eq. (3) subject to large relative errors. The larger  $\Delta[\text{CO}_2]$  threshold reduces the  $K_{\text{CO}_2}$  range further, to about  $-0.1$  to  $0.4 \text{ m}^2 \text{ s}^{-1}$ . The positive side of this range is similar to the range of momentum diffusivities and therefore considered realistic. The negative side is due to sign mismatches between CO<sub>2</sub> fluxes and gradients. Most of these occur around the morning and evening transitions, indicating that at such times the surface fluxes and surface-layer gradients are not in equilibrium, and that the application of a simple flux-gradient concept is then not appropriate. All runs with negative  $K_{\text{CO}_2}$  are thus excluded from further analysis, in addition to the runs with  $\Delta[\text{CO}_2] < 2.4$  ppm.

Turbulent diffusivities are positively correlated with wind speed; for  $K_m$  this is evident from the dependence on  $u_*$  in Eq. (2). In Fig. 4, it is apparent that filtering with the larger  $\Delta[\text{CO}_2]$  threshold removes almost all values measured at higher wind speeds. The higher the wind speed, the better the turbulent mixing, and consequently, the smaller the vertical gradients of any scalar variables. As these gradients approach their resolution limits, the GGR method becomes inaccurate. Here, a minimum threshold for  $\Delta[\text{CO}_2]$  of 2.4 ppm implies a maximum wind speed of approximately  $5 \text{ m s}^{-1}$ .

### 3.2.3 Filter thresholds and data yield

Of over 22 000 runs with measured  $\Delta[\text{CO}_2]$ , 9193 for the IFR site and 6912 for the U UW site passed the  $\Delta[\text{CO}_2]$  threshold

value. The higher rejection rate for the U UW site is consistent with CO<sub>2</sub> fluxes and gradients at that site being generally closer to zero than at the IFR site. A few hundred runs were eliminated during grazing events. Further, since the CO<sub>2</sub> fluxes for runs with  $\sigma_w < 0.12 \text{ m s}^{-1}$  were excluded and replaced with gap-filled values, such runs were not used for the GGR method. Of the remaining runs, 6 % at the IFR and 13 % at the U UW site had to be discarded because of negative  $K_{\text{CO}_2}$ , leaving 3757 and 2424 runs, respectively. The overall relative data yield of the GGR method was thus 17 % at the IFR site and 11 % at the U UW site.

### 3.2.4 Footprint considerations

For the CO<sub>2</sub> fluxes measured by eddy covariance, the footprints were computed with the tool of Neftel et al. (2008), which implements the model of Kormann and Meixner (2001). The footprint contributions from the target surface were found  $> 90$  % most of the time, at both sites (Hunt et al., 2016).

Flux footprints depend on measurement height. For the trace gas fluxes using the GGR method, the effective measurement height must be somewhere between the heights of the two intakes (0.76 and 1.96 m). This intermediate height, regardless of how exactly it is specified, is lower than the eddy-covariance measurement height (1.86 m); hence, the footprint contributions of the target surface to the CH<sub>4</sub> and N<sub>2</sub>O fluxes are even larger than for the eddy fluxes. Compared to the overall uncertainty of the fluxes, the footprint contributions from areas outside the target surface are thus considered negligible, and no wind-direction filtering was applied to the data.

### 3.2.5 Diurnal courses and daily means of fluxes

An example of CH<sub>4</sub> and N<sub>2</sub>O fluxes obtained with the GGR method is shown in Fig. 5, along with wind speed. Some negative flux values occur, and since negative diffusivities have been explicitly excluded, these must be due to positive (upwards-increasing) gradients. Data yield is higher at the IFR site, as already noted to be the case throughout. At both sites the range of N<sub>2</sub>O fluxes is fairly consistent from one day to the next, the daily mean N<sub>2</sub>O fluxes are positive for all days shown and the scatter is of the same magnitude as the mean. For the CH<sub>4</sub> fluxes, the picture is less consistent: on some days (e.g. 14 February) the range is much larger than on others (e.g. 17 February), the large range includes positive and negative fluxes, and on days with such a large range the scatter is much larger than the mean and makes the latter's value highly uncertain. The days with large scatter tend to be windier than those without; therefore, in part the large scatter may be due to relatively small CH<sub>4</sub> gradients, near the FTIR resolution limit, being multiplied with large diffusivities, which in effect amplifies the random error of the gradient measurements. This can of course occur



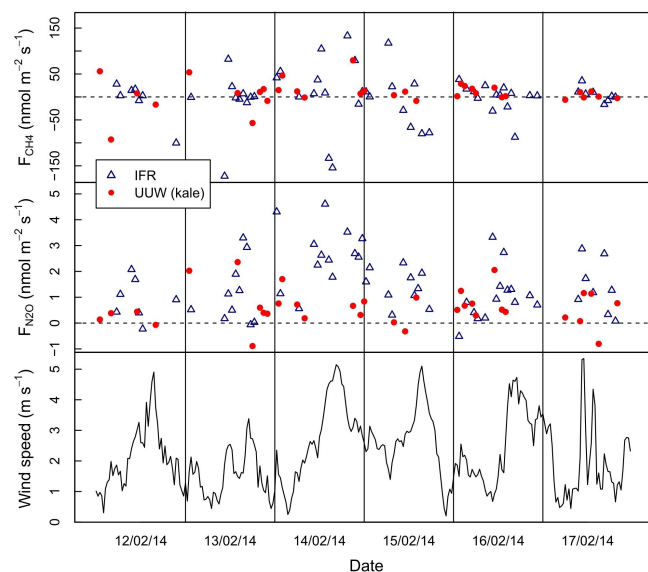


**Figure 5.** Half-hourly fluxes of CH<sub>4</sub> (top) and N<sub>2</sub>O (middle) at the two sites, obtained with the GGR method, as well as wind speed (bottom), for an example period.

for N<sub>2</sub>O, too. Another possibility, more specific to CH<sub>4</sub>, is the existence of large sources, such as grazing animals, in nearby paddocks. Temporal variations of wind direction may cause the emissions plumes from such sources to contaminate the air sampled from either intake. Since the intakes are sampled sequentially, the sign and magnitude of the contamination effect on the gradient would then depend strongly on the exact timing of such a plume's passage. Lacking detailed information of cattle presence in paddocks other than the target paddocks, we do not have any objective criteria to decide which CH<sub>4</sub> flux records are contaminated. Hence, we only apply a crude outlier filter, by removing fluxes that fall outside  $\pm 5$  times the SD of the whole data set.

Assuming that no strong diurnal courses are expected for either CH<sub>4</sub> or N<sub>2</sub>O fluxes, and that the within-day variability of both is largely random, we assess seasonal variability from daily means and their standard errors (SE). Days with fewer than four valid runs were excluded. Daily fluxes were obtained on 59 and 38 % of all days for the IFR site and the UUW site, respectively. These were spread reasonably evenly across all seasons (Figs. 6, 7), with the lowest coverage in June (early winter).

At both sites, daily means of CH<sub>4</sub> fluxes using the GGR method were generally small compared to their SE and thus often not significantly different from zero. No seasonal trends were discernible, and no quasiperiodic patterns that could be associated with the rotational grazing, either. The median daily CH<sub>4</sub> fluxes were 3.7 and 4.9 nmol m<sup>-2</sup> s<sup>-1</sup> at the IFR site and the UUW site, respectively, indicating small net emissions overall; the median SE of these daily fluxes were 8.2 and 7.8 nmol m<sup>-2</sup> s<sup>-1</sup>, respectively.

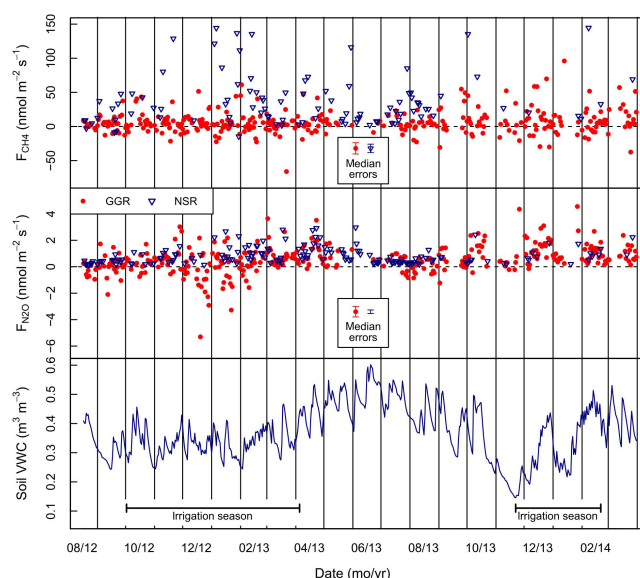


**Figure 6.** Daily mean fluxes of CH<sub>4</sub> (top) and N<sub>2</sub>O (middle) at the IFR site, using the GGR method (dots) and using the NSR method (triangles). In these two panels, error bars in insets indicate for each method (GGR left, NSR right) the median of the standard error of the daily mean flux. Bottom panel: volumetric water content at 5 cm depth.

Daily means of N<sub>2</sub>O fluxes from the GGR method also occurred with either sign (middle panels of Figs. 6, 7); however, after 15 October 2013, when the modified switching cycle (12 min per intake) was used, negative daily fluxes became rare. At the IFR site, daily N<sub>2</sub>O fluxes spanned the range  $\pm 5$  nmol m<sup>-2</sup> s<sup>-1</sup>, but the majority of values were of a positive sign. The median daily flux was 0.52 nmol m<sup>-2</sup> s<sup>-1</sup>. This was greater than the median of the associated SE values, of 0.39 nmol m<sup>-2</sup> s<sup>-1</sup>, and thus indicated significant net emissions overall. At the UUW site, daily N<sub>2</sub>O fluxes ranged from  $-1.2$  to  $1.9$  nmol m<sup>-2</sup> s<sup>-1</sup>. The median flux was 0.28 nmol m<sup>-2</sup> s<sup>-1</sup>, and the median SE of the daily fluxes was 0.29 nmol m<sup>-2</sup> s<sup>-1</sup>. As with CH<sub>4</sub>, it was difficult to detect any seasonal trends, except for a slight tendency for larger variability throughout the irrigation seasons (which are largely identical with the seasons of N inputs from grazing and fertiliser application). In particular, there were no obvious responses of N<sub>2</sub>O fluxes to soil moisture (bottom panels of Figs. 6, 7).

### 3.3 NSR method

#### 3.3.1 NSR regressions

For the NSR method, linear regression slopes for N<sub>2</sub>O and CH<sub>4</sub> mole fractions vs. CO<sub>2</sub> mole fraction were determined for each night in which runs with  $\sigma_w < 0.12$  m s<sup>-1</sup> occurred (including only these runs in the regression). To be reliable, the linear relationship must have a high  $R^2$  and must be

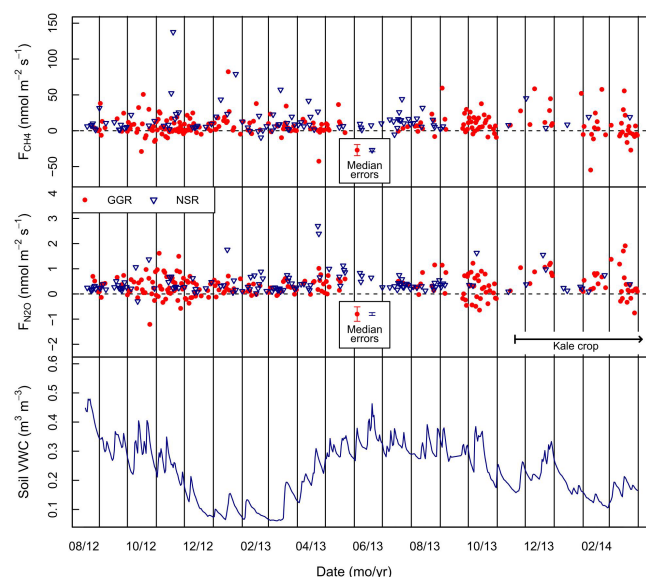


**Figure 7.** As Fig. 6 but for the UYW site.

based on a sufficient number of runs ( $n$ ). Therefore, minimum thresholds for both parameters are required. During most low-turbulence nights, the regressions of [N<sub>2</sub>O] vs. [CO<sub>2</sub>] had  $R^2$  values greater than 0.7, at both sites. There was no relationship between  $R^2$  and  $n$ , except that the scatter in  $R^2$  seemed to increase with decreasing  $n$  (not shown). For [CH<sub>4</sub>], the  $R^2$  values of the NSR regressions vs. [CO<sub>2</sub>] tended to be lower than for [N<sub>2</sub>O]; their majority spread between 0.3 and 0.8, again irrespective of  $n$ . Lacking any obvious cut-off values for  $R^2$  and  $n$ , their choices must be made pragmatically by balancing the reliability of the individual regression (in favour of high thresholds) against the statistical power of including a large number of nights (in favour of low thresholds). We used a minimum  $R^2 = 0.4$  and a minimum  $n = 4$ , which leaves about 29 % of nights available for CH<sub>4</sub> and about 48 % for N<sub>2</sub>O.

Figure 8 shows the evolution of the NSR regression slopes over time. For three-quarters of the year, the N<sub>2</sub>O vs. CO<sub>2</sub> slopes show mainly short-term variations, but hardly any seasonal trend; yet during the colder months May to July they increase to 3 to 5 times higher levels. Both the short-term and the seasonal variations are very similar for the two sites. The CH<sub>4</sub> vs. CO<sub>2</sub> slopes are less well correlated between the two sites, and short-term variations dominate throughout, while seasonal trends are absent.

### 3.3.2 Nocturnal CO<sub>2</sub> fluxes

The NSR method requires one representative CO<sub>2</sub>-flux value for each night. This value was obtained as the mean of the half-hourly fluxes from the gap-filled EC records. As a quality check on the gap-filling, Fig. 9 compares the night-mean EC fluxes from the complete, gap-filled record with night-

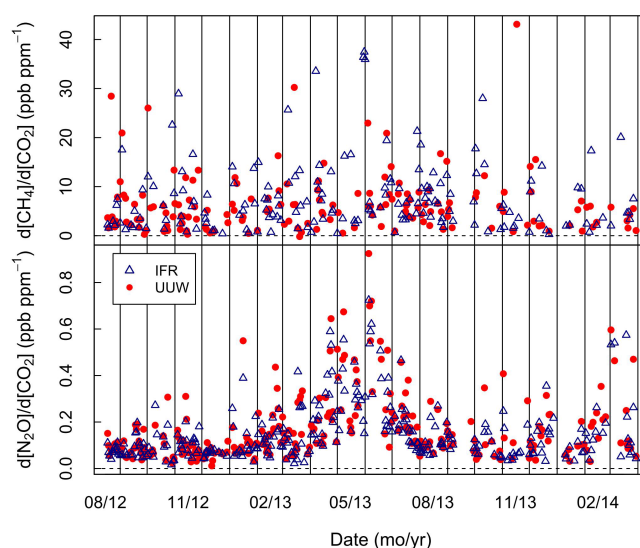


**Figure 8.** Temporal variation of the slopes of the linear regressions between CH<sub>4</sub> and CO<sub>2</sub> (top panel) and between N<sub>2</sub>O and CO<sub>2</sub> (bottom panel), for both sites.

means obtained from measured CO<sub>2</sub> fluxes using only runs with  $\sigma_w > 0.12 \text{ m s}^{-1}$  (including only nights with at least nine such runs available). At both sites, and for all seasons, the two time series track each other well. The measured-only series appears at times more scattered, but no systematic differences occur.

For the period from 23 September 2013 to 31 March 2014, mean nocturnal CO<sub>2</sub> fluxes at the IFR site were also computed from the respiration chamber data. The ratio of the night-mean EC fluxes to night-mean chamber fluxes was on average  $0.87 (\pm 0.34 \text{ SD})$ , and agreement was generally best for the first few days following grazing events (matched by cutting of the grass in the chambers).

### 3.3.3 Footprint considerations and nocturnal fluxes of CH<sub>4</sub> and N<sub>2</sub>O

From footprint models it is known that the source area influencing a flux measurement in the atmospheric surface layer has a larger extent when stratification is stable than when it is unstable (Schmid, 1994; Kormann and Meixner, 2001). During nocturnal low-wind periods, stable stratification prevails; therefore, comparatively large source areas can be expected for the NSR method. Further, the source area influencing a mole-fraction measurement extends farther than that influencing a flux measurement (Schmid, 1994). Since the NSR method combines measurements of a flux, that of CO<sub>2</sub>, with measurements of the changes of a mole fraction, that of  $\chi$ , over time, it can be hypothesised that its effective source area is somewhat larger than that of a direct flux measurement (e.g. by eddy covariance or the GGR method). For our set-up geometry (Fig. 1), NSR measurements at the IFR site

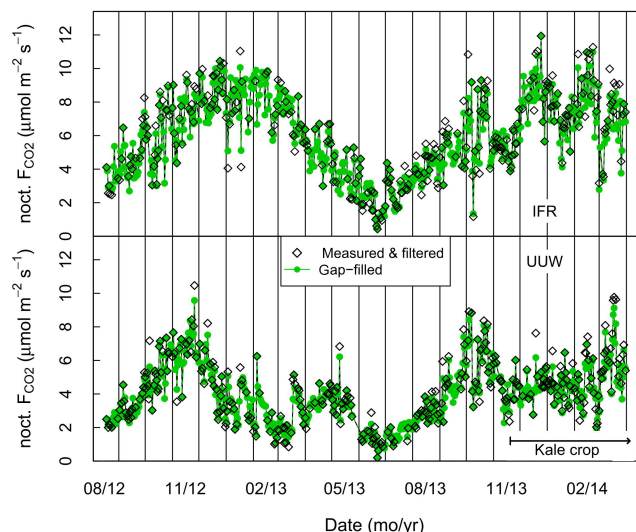


**Figure 9.** Nocturnal CO<sub>2</sub> emission rates from the IFR site (top) and the UUW site (bottom). Each point is a whole-night average, obtained either only from measured values during periods with sufficient turbulence ( $\sigma_w > 0.12 \text{ m s}^{-1}$ ; open diamonds), or from the complete gap-filled data set (solid dots).

could in part be influenced by conditions over the dryland area, for wind directions either side of north, from 284 to 76°. Similarly, NSR measurements at the UUW site could in part be influenced from either of the two irrigated circles to the south and west, hence for any wind direction between 93 and 321°. Table 2 shows the differences in the median nocturnal fluxes between including and excluding periods with winds from the specified directional sectors, as well as the number of nights ( $N$ ) contributing to each median flux. The wind-direction filter is applied on a half-hourly basis, together with the low-turbulence filter ( $\sigma_w < 0.12 \text{ m s}^{-1}$ ), prior to the NSR regression and the filtering for  $R^2 > 0.4$  and  $n \geq 4$ .

One effect of the exclusion of unsuitable wind directions is a considerable reduction of  $N$ , by about half. In addition (not shown), the number of runs contributing to each night,  $n$ , is also on average reduced. Of all nocturnal half-hours with low turbulence, 63 % had unsuitable wind direction for the IFR site, and 67 % for the UUW site. The reason for such high exclusion rates is a predominance of wind from the north-west sector, due to katabatic flow from the Southern Alps. Unfortunately, those wind directions that were unsuitable at both sites (284 to 321°) were also the most common.

At the IFR site, the median CH<sub>4</sub> flux with wind-direction filtering is 3 % greater than without, and the median N<sub>2</sub>O flux with filtering is 5 % greater than without. At the UUW site, wind-direction filtering reduces the median CH<sub>4</sub> flux by 38 % and the median N<sub>2</sub>O flux by 27 %. The effect of the filter at this site appears large enough to justify its application, despite the considerable reduction in data yield.

At both sites and for both gases, the means of the nocturnal fluxes were greater than their medians, with SDs between

0.76 and 1.3 times the mean values. Due to these large relative SDs, the means were quite sensitive to the presence (or exclusion) of outliers and are for that reason not reported in Table 2.

### 3.3.4 Uncertainty of the CH<sub>4</sub> and N<sub>2</sub>O fluxes

The uncertainty of the NSR regression slope is expressed as its SE. In relative terms, this ranged from 2 to 80 % of the regression slope, for both sites and gases. For CH<sub>4</sub>, the median relative errors of the slopes were 29 % at both sites. For N<sub>2</sub>O, these median errors amounted to 20 % at the IFR site and 17 % at the UUW site.

The uncertainty of the nocturnal CO<sub>2</sub> fluxes, from the gap-filled EC data, was specified as the SEM for each night. This includes the contributions from random measurement error and temporal variability during the night. Expressed as a relative error, it ranged from 0.4 to 33 % of the flux but rarely exceeded 15 %. The median relative errors were 4.2 and 4.3 % for the IFR site and the UUW site, respectively. The number of runs per night contributing to the mean had a median of 21, at both sites. Multiplying the median relative error of the night-mean flux with  $21^{1/2}$ , the typical relative error of the individual half-hour flux is obtained as 19 and 20 % for the IFR site and the UUW site. This appears realistic, since nocturnal CO<sub>2</sub>-flux errors in windy conditions are often estimated to be of the order of 20 % (Moncrieff et al., 1996).

We thus estimate the SEM of the nocturnal CH<sub>4</sub> and N<sub>2</sub>O fluxes by combining the SEM of the nocturnal CO<sub>2</sub> fluxes with the SE of the regression slopes (using standard root mean square propagation). The fluxes and their SEM are shown in Figs. 6 and 7, along with their counterparts from the GGR method.

## 3.4 Combination of GGR and NSR methods

### 3.4.1 Comparison of the two methods

The GGR method provided a higher yield of daily flux values for CH<sub>4</sub> and N<sub>2</sub>O than the NSR method, and also the larger day-to-day variability (Figs. 6, 7). The N<sub>2</sub>O fluxes from the NSR method generally followed the trends of those from the GGR method well, at timescales of a few days or longer. The same was true for the CH<sub>4</sub> fluxes at the UUW site (Fig. 7), with the exception of a couple of high outliers in November 2012 and January 2013. For N<sub>2</sub>O, the median fluxes from the two methods were also in good agreement (for NSR 23 and 4 % greater than for GGR at the IFR site and the UUW site, respectively).

About half of the CH<sub>4</sub> fluxes from the NSR method at the IFR site were considerably greater than those from the GGR method, while the other half agreed well with the trend of the latter (Fig. 6). The likely cause of the discrepancies for CH<sub>4</sub> is the presence of the cattle herd elsewhere in the irrigated circle, acting as a strong source of CH<sub>4</sub> that was not

**Table 2.** Medians of nocturnal fluxes computed with the NSR method, as well the number of nights ( $N$ ) contributing to the median, for two wind-direction selections: all included or unsuitable ones excluded. Directions are considered unsuitable for the IFR site when the dryland area is upwind, and unsuitable for the UUW site when either of two neighbouring irrigated circles is upwind. See text for specification of the directional sectors.

Trace gas	Site	All wind directions		Unsuitable directions excluded	
		median flux (nmol m <sup>-2</sup> s <sup>-1</sup> )	$N$	median flux (nmol m <sup>-2</sup> s <sup>-1</sup> )	$N$
CH <sub>4</sub>	IFR	25.6	172	26.3	101
CH <sub>4</sub>	UUW	14.0	164	8.73	96
N <sub>2</sub> O	IFR	0.604	293	0.637	165
N <sub>2</sub> O	UUW	0.396	279	0.289	131

uniformly spread across the pasture surface in the same way as the sources of CO<sub>2</sub> and N<sub>2</sub>O. During stable surface-layer stratification, the CH<sub>4</sub> (and CO<sub>2</sub>) emitted by the cattle would accumulate in the surface layer and, with mean wind close to zero, slowly spread in all directions until, eventually, being moved and dispersed by an intermittent flow event.

Without records of grazing events in paddocks other than those two containing our instrument sites, there are no clear criteria to decide in which nights the NSR estimates of CH<sub>4</sub> flux are significantly biased by cattle emissions and in which they are not. Histograms of the CH<sub>4</sub> fluxes for both sites (not shown) suggest that fluxes greater than 80 nmol m<sup>-2</sup> s<sup>-1</sup> are very likely outliers due to cattle emissions. We thus remove these from further analysis. This reduces the number of nights, of 101 and 96 for the IFR site and UUW site (Table 2), to 88 and 95, respectively. However, the possibility remains that further nights are affected and that the NSR estimates for CH<sub>4</sub> fluxes may be overestimated in these.

### 3.4.2 Construction of emissions budgets

The time series of daily CH<sub>4</sub> and N<sub>2</sub>O fluxes can be used to construct emissions budgets for longer periods, such as seasons or years. For this, we wish to make good use of the two complementary methods. A simple approach is to take separate means for the GGR method and the NSR method and then average these, giving equal weight to each method (we shall call this the “combined” approach). An alternative approach can be described as follows: first, average GGR and NSR means on a daily basis for each 24 h period in which both estimates are available; then, for 24 h periods in which only one method produced a valid mean flux, use that flux; finally, take the overall mean of this merged time series (we shall call this the “merged” approach). The merged approach gives more weight to the method with the greater data yield.

We explore these two approaches for the first year of the data set (17 August 2012 to 16 August 2013). With both approaches, we estimate the uncertainty by propagating the SE of all day means/night means into an SE value for the annual mean flux. The results are summarised in Table 3. All flux values in the table are positive, indicating net annual emis-

sions of the two trace gases. Data yields ( $N$ ) are included in the table; for the combined approach no  $N$  column is given because the individual  $N$  for the GGR and NSR methods apply.

For CH<sub>4</sub> at the IFR site, the NSR method estimates 5 times greater emissions than the GGR method, despite the outlier filtering described above. Since the data yield of the GGR method was 3 times greater, the relative weighting of the two methods matters; consequently, the combined approach results in an emissions estimate that is 1.6 times that of the merged approach. By contrast, for CH<sub>4</sub> at the UUW site, GGR and NSR estimates differ by less than a factor 2; consequently, the combined and merged approach agree within 10 %.

For N<sub>2</sub>O at the IFR site, the annual NSR mean exceeds the annual GGR mean by a factor of 2.6. This is a considerably greater difference than was found for the medians (of this year as well as of the whole data set). The GGR mean includes 62 % of the days of the year, while the NSR mean is based on 38 % of all nights. Both data sets are evenly spread across the seasons (Fig. 6). The GGR data set contains a surprisingly large number of negative daily values in December 2012 and January 2013 while the NSR data set does not contain negative values, and the different annual means for the two methods are largely caused by this. The combined approach results in an annual flux estimate that is 23 % greater than the estimate from the merged approach, in which the NSR data have less weight.

For N<sub>2</sub>O at the UUW site, the annual NSR mean exceeds the annual GGR mean by 57 %. Again, this is a greater difference than that for the medians. The data yields for both methods are smaller than at the IFR site, but roughly in the same proportion with each other. The combined approach results in a 5 % greater annual flux estimate than the merged approach, and the ranges indicated by the propagated daily SE are marginally overlapping. Again, the GGR data set contains some negative daily means (while the NSR data set does not); these occurred mostly in October–November 2012, not at the same time as for the IFR site.

**Table 3.** Estimates of mean annual fluxes, for the period 17 August 2012 to 16 August 2013, from four approaches: GGR method, NSR method, mean of the annual means of GGR and NSR, and annual mean of daily values obtained from merging the two methods. Numbers in parentheses are error estimates from propagation of daily standard errors. *N* is the number of nights contributing.

Trace gas	Site	GGR method		NSR method		GGR and NSR means combined	GGR and NSR merged daily	<i>N</i>
		mean flux (nmol m <sup>-2</sup> s <sup>-1</sup> )	<i>N</i>	mean flux (nmol m <sup>-2</sup> s <sup>-1</sup> )	<i>N</i>	mean flux (nmol m <sup>-2</sup> s <sup>-1</sup> )	mean flux (nmol m <sup>-2</sup> s <sup>-1</sup> )	
CH <sub>4</sub>	IFR	4.7 (0.92)	224	24.3 (1.22)	77	14.5 (0.76)	8.9 (0.79)	259
CH <sub>4</sub>	UUW	6.7 (1.05)	147	12.9 (0.77)	84	9.8 (0.65)	8.9 (0.79)	201
N <sub>2</sub> O	IFR	0.32 (0.034)	225	0.83 (0.021)	137	0.58 (0.020)	0.47 (0.024)	273
N <sub>2</sub> O	UUW	0.30 (0.032)	147	0.47 (0.018)	108	0.38 (0.018)	0.36 (0.022)	211

## 4 Discussion

### 4.1 Performance of the GGR method

The GGR method and the NSR method exploit complementary data sets: for the former, only runs are used in which a set turbulence threshold is exceeded, for the latter only runs in which the opposite is true. The data yield of each method is thus dependent on the general wind climate of the site. However, each method also requires careful screening with other suitability criteria. For the GGR method, we have demonstrated that the main one is to ensure that the mole-fraction gradients of the reference gas (here CO<sub>2</sub>) are a few times larger than instrument resolution, in order to contain random scatter within tractable limits. An implication of this requirement is that very high wind speeds tend to be less suitable than moderate wind speeds, because the former dilute emitted gases more quickly and thus reduce their gradients. The exact choice of filtering criteria must balance reliability (constraining random error) with availability (obtaining enough data coverage).

Even with appropriate filtering, run-to-run variability of the GGR method is large, because the random errors of three measured variables (two gas mole-fraction gradients and the reference gas flux) combine, and partly because the two gas mole fractions are measured sequentially, not simultaneously (although usage of ballast volumes reduces the effects of timing mismatch somewhat). The random error of a daily mean flux depends, then, on the number of acceptable runs, and may thus be large on some days and small on others. In our experiment, we obtained acceptable daily mean fluxes for approximately 40 % of all days at one site and 60 % at the other. This was sufficient for adequate coverage of all seasons and the estimation of annual budgets of gas emissions.

The large uncertainty of individual runs found with the GGR method is similar to that found with the momentum-based aerodynamic method (Phillips et al., 2007). The data yield of the former is probably smaller than that of the latter, because suitably large [CO<sub>2</sub>] gradients (required for GGR) may occur somewhat less often than reliable mea-

surements of friction velocity (required for the aerodynamic method). However, the GGR method avoids any assumptions on Schmidt number and stability dependence and its diffusivity estimates are therefore more defensible for the purpose of computing trace gas fluxes.

For both trace gases, negative flux values (uptake) were occasionally observed with the GGR method. In the case of CH<sub>4</sub>, the negative fluxes were spread across all seasons, at both sites. They are thus considered as manifestations of the large random variability. By contrast, negative fluxes of N<sub>2</sub>O were occasionally clustered in certain periods. These cluster periods were not synchronous at the two sites. During these, the mole-fraction gradients with reversed sign occurred consistently over many successive cycles, suggesting that they had a true cause, rather than occurring randomly. However, the NSR method did not indicate N<sub>2</sub>O uptake during these periods. While we cannot rule out the possibility that the negative N<sub>2</sub>O fluxes from the GGR method were artefacts, we have no indication from the data themselves, or our records of instrument operation and farm management, why they might have been.

### 4.2 Performance of the NSR method

The NSR method relies on the occurrence of nocturnal calm periods of a few hours duration. Such periods do not occur every night. When they do, the method is technically robust, since the gas mole-fraction changes over time tend to be large and can be well resolved. A crucial assumption of the NSR method is the co-location, in space and time, of the sources or sinks of the trace gas of interest and the reference gas. In our experiment, the results for N<sub>2</sub>O were very consistent with those from the GGR method, so we conclude that for N<sub>2</sub>O and CO<sub>2</sub> over pasture this assumption holds well enough, as it did in the pioneering experiment of Kelliher et al. (2002). The results for CH<sub>4</sub> were less consistent, and we attribute that to the presence of cow herds in the larger surroundings of the measurement site. These constituted strong additional sources, of both CH<sub>4</sub> and CO<sub>2</sub> but with a very different emissions ratio to that valid for the pasture, and therefore occa-



sionally (depending on intermittent winds) impacting on the correct retrieval of the latter.

The footprint of the NSR method has a rather large spatial extent, compared to the GGR method. Because of the requirement of co-location of sources/sinks, one needs to exclude periods when the extension of the target surface in the wind direction is too short. In our experiment, the prevalence of katabatic flow from a certain directional sector led to the exclusion of 40 % or more of otherwise suitable calm nights. Such high exclusion rates could be avoided by maximising the fetch in the main regional upslope direction (but in our case, this would have conflicted with the requirements of the dual-site set-up and was thus impossible). Here, the NSR method provided fewer night-mean flux estimates than the number of daily means obtained with the GGR method; however, this does not need to be the case in general, since the data yield of both methods depends on local wind climate and footprint considerations.

The NSR method requires reliable flux estimates for the reference gas. Here, we have explored a novel approach to this end, by using gap-filled long-term time series of CO<sub>2</sub>-flux records, instead of chamber measurements. Hence, the actual flux values used for the NSR-suitable night-time periods were modelled, but strongly based on measured fluxes in the surrounding windier periods. They were validated against chamber measurements and found to provide adequate estimates of the nocturnal mean respiration flux, with a relative uncertainty that was usually smaller than that of the NSR regression slope and therefore did not impact negatively on the success of the NSR method.

### 4.3 Annual means of CH<sub>4</sub> and N<sub>2</sub>O emission rates

Either of the two methods, GGR and NSR, can provide annual budget estimates of trace gas fluxes on its own, provided that these fluxes do not undergo strong systematic diurnal variations. If they did, then biases would be likely, since the GGR method yields more data during the day than at night and the NSR method is explicitly nocturnal only. We thus strongly recommend to combine the two methods. As they are applicable in mutually exclusive conditions (well-developed turbulence and calm, respectively), their combination optimises data usage.

We tested two approaches to combine the GGR and NSR results: either combining their separate annual means, or merging the two time series into one before computing a joint annual mean. Ideally, the two approaches should not differ by much. Here, we found that to be the case for the CH<sub>4</sub> fluxes at the UUW site. However, when the results from the GGR and NSR methods show systematic differences, then some operator judgment is required whether that reflects true day–night differences of the fluxes or whether one of the two methods is likely to be biased. In the former case, combining GGR and NSR means would be adequate, as that would give similar weights to daytime and night-time data. In the latter case,

the likely cause of bias needs to be assessed and the decision how to weigh the GGR and NSR results must be based on that assessment.

For the CH<sub>4</sub> results at the IFR site, we suspect that the mean fluxes from the NSR method are overestimated in many nights, due to the presence of cows emitting CH<sub>4</sub> elsewhere on the irrigated-pasture circles. Thus, for CH<sub>4</sub> we decide to give high weight to the GGR method, by using the results from the merged approach. This yields identical emission rates of 8.9 ( $\pm 0.79$ ) nmol m<sup>-2</sup> s<sup>-1</sup> for the two sites (Table 3). If we used the combined approach instead, the mean emission rate from the IFR site would appear as the significantly greater one.

For annual N<sub>2</sub>O fluxes, the mean from the NSR method was somewhat greater than that from the GGR method, at both sites. We found the differences to originate mainly from certain periods in which the GGR method repeatedly indicated negative fluxes, while the NSR method did not. It is possible that during these periods the pasture acted as an N<sub>2</sub>O sink during daytime and as a source during the night; Hörtnagl and Wohlfahrt (2014) observed such behaviour in the spring seasons of two consecutive years and in autumn for one of these years. Therefore, we decide to use the combined approach for N<sub>2</sub>O, giving equal weight to the GGR method and the NSR method despite the greater data yield of the former. Considering high N<sub>2</sub>O fluxes as undesirable, this decision errs on the side of caution and produces somewhat greater emission rates than would be obtained with the merged approach. These emission rates are 0.58 ( $\pm 0.020$ ) and 0.38 ( $\pm 0.018$ ) nmol m<sup>-2</sup> s<sup>-1</sup> for the IFR and the UUW site, respectively (Table 3). Hence, the emission rates from the IFR site were significantly greater than those from the UUW site, by 53 %. This is in line with expectations, given the greater N inputs from fertiliser application and excreta deposition at the IFR site.

### 4.4 CH<sub>4</sub> fluxes from managed grasslands

Agricultural soils, when not waterlogged, are expected to be weak sinks for CH<sub>4</sub> (Smith et al., 2003), and chamber studies have tended to confirm this expectation. For example, Imer et al. (2013) reported net uptake rates for three managed ungrazed grassland sites in Switzerland; Savage et al. (2014) found annual CH<sub>4</sub> uptake of 0.2 g C m<sup>-2</sup> for an alfalfa field in North Dakota, using year-round auto-chamber sampling. In New Zealand, Li and Kelliher (2007) reported net uptake rates of 0.14 and 0.05 g C m<sup>-2</sup> yr<sup>-1</sup> for a well-drained and a poorly drained dairy-pasture soil, situated 300 m apart. By contrast, the results reported here indicate both the IFR and the UUW site to be CH<sub>4</sub> sources, with similar annual net emissions (for the year starting 17 August 2012) of 3.4 g C m<sup>-2</sup>. Even if one discarded the NSR results completely on suspicion of CH<sub>4</sub> contamination by animal herds in the wider surroundings, the GGR data sets alone still have positive means and medians, at both sites. Since the daytime



footprint extensions for the GGR method were of the order of 300 m or less, we can be confident that the GGR results were generally representative for pasture surfaces free of grazing animals.

Other micrometeorological studies of grasslands are useful to compare with our CH<sub>4</sub> results only where grazing events were excluded from the data, where the soils were not peaty and where the footprint contained no open-water surfaces. Using eddy covariance, Hörtnagl and Wohlfahrt (2014) found, at an alpine meadow that was cut three times per year, CH<sub>4</sub> emission rates of the order of 1 nmol m<sup>-2</sup> s<sup>-1</sup>; these were very consistent throughout all snow-free seasons. For a grassland site after restoration, Merbold et al. (2014) reported annual CH<sub>4</sub> emissions of 3.53 g C m<sup>-2</sup>, very similar to our two sites, and daily mean emissions were in the majority of a positive sign in every month. Griffith et al. (2002), using the flux-gradient method over lucerne pasture in New South Wales, reported mean and median daytime fluxes of 2.95 and 2.85 nmol m<sup>-2</sup> s<sup>-1</sup>, and even though these were not significantly different from zero due to the short duration of that experiment (3 weeks), the sign and magnitude agree with those from the other micrometeorological studies. It appears that net CH<sub>4</sub> emissions from managed grasslands are not uncommon, which is at odds with those chamber experiments that demonstrated CH<sub>4</sub> oxidation. A possible explanation is that frequent N fertilisation inhibits the oxidation process and/or stimulates CH<sub>4</sub>-producing microbes in the soil (Price et al., 2004). Li and Kelliher (2007) found that urine application reduced net CH<sub>4</sub> uptake significantly, both for a well-drained and a poorly drained soil. We note, though, that the net uptake rates observed for each of their treatments were at least 1 magnitude smaller than the mean emission rates at our sites. The same is true for an experiment with intact soil cores from European sites (Schaufli et al., 2010), where the cropland and grassland soils showed CH<sub>4</sub> fluxes smaller than 0.06 nmol m<sup>-2</sup> s<sup>-1</sup>, some with net uptake and some with net emissions, and without dependence on soil moisture or temperature. Another possible factor favouring CH<sub>4</sub> emissions may be the soil compaction caused by intensive grazing events, provided that leads to an increased occurrence of anaerobic microsites in the soil. Whatever the exact mechanisms, the field-scale CH<sub>4</sub> flux measurements here and elsewhere suggest that on managed pastures, CH<sub>4</sub> oxidation rates in the soil can be overwhelmed by concurrent emission processes.

#### 4.5 N<sub>2</sub>O emissions and nitrogen inputs

The time series of N<sub>2</sub>O fluxes in Figs. 6 and 7 are, overall, relatively steady. In Fig. 6, there is no quasiperiodic pattern that would indicate a response to events of strong N input (grazing or fertilisation). There is also an almost complete lack of strong episodic events. Such events have often been reported to closely follow rainfall or irrigation events (e.g. van der Weerden et al., 2013), and they are found to

occur in a relatively narrow range of soil moisture that is site-specific. Balaine et al. (2013) presented evidence that the driving variable for peak N<sub>2</sub>O emissions is the relative soil gas diffusivity. Here, at the IFR site throughout the milking season, it appears that VWC was generally too low to reach the conditions required for peak emissions. The highest VWC occurred over winter 2013 (June to August), generally between 0.4 and 0.55 m<sup>3</sup> m<sup>-3</sup> (equivalent to 60 and 83 % water-filled pore space, respectively, given a porosity of 66 % in the soil layer from 0 to 10 cm depth). During this winter period, the N<sub>2</sub>O fluxes appeared particularly small and steady, at 0 to 0.5 nmol m<sup>-2</sup> s<sup>-1</sup>. This was also a period in which no fertilisation or grazing events occurred. The relative steadiness of N<sub>2</sub>O emission rates throughout all seasons is probably largely due to the well-drained soil. This feature distinguishes this intensively managed pasture site from others (Phillips et al., 2007), where emissions were of a more episodic nature and more obviously responding to irrigation events.

In Table 4, we relate the N<sub>2</sub>O emissions at the IFR site to the N inputs, for the same year as in Table 3. The N inputs are obtained as follows. Fertilisers were applied by a certified commercial contractor, who recorded the amounts per area; we assume a relative error of 7 % from expert judgment. The N inputs from cattle excreta can be accounted for as the N intake by the animals reduced by the N retention in liveweight and the N content of milk produced, under the assumption that all excreted N is returned to the irrigated-pasture circle either in situ as dung and urine or by effluent application. Following Hunt et al. (2016), the dry-matter intake of the cattle herd for the 2012/13 milking season was 1.167 (±0.026) kg m<sup>-2</sup> (90 % grazed pasture, 10 % barley supplements). With an N content of 2.7 (±0.2) % for ryegrass/clover pasture (Mills and Moot, 2010), the N intake amounted to 31.5 (±2.4) g N m<sup>-2</sup>. The total liveweight gain of the herd over the milking season was estimated as 52 200 kg, based on national statistics (DairyNZ, 2013) and the age structure of the herd. Dividing by the total grazed area of the farm (328 ha), and assuming an N content of 3.6 % for meat (AMC, 2014), the N retention in liveweight per pasture area was 0.57 g N m<sup>-2</sup> (1.8 % of N intake). The milk production of the farm for 2012/13 was 3.96 × 10<sup>6</sup> L. Assuming that the milk contained 5.8 (±0.5) g N L<sup>-1</sup> (Woodward et al., 2011), the amount of N exported in milk was 7.0 (±0.6) g N m<sup>-2</sup> (22 % of N intake). The amount of N returned in excreta thus results as 23.9 (±2.5) g N m<sup>-2</sup>.

The figure for the N<sub>2</sub>O emissions in Table 4 comes from the combined approach (see Sect. 4.3), converted from molar units (0.58 nmol m<sup>-2</sup> s<sup>-1</sup>) to mass units and integrated over a year, yielding 0.51 g N m<sup>-2</sup>. The uncertainty of this value is assumed as 10 % in relative terms. This is greater (about 3 times) than the propagated SE in Table 3, partly to account for the mismatch between approaches as discussed above, and partly to allow for the possibility that the spatial variability in the whole irrigated circle may have been larger

**Table 4.** Nitrogen budget terms for the IFR site for the year 17 August 2012 to 16 August 2013. The N<sub>2</sub>O emissions value is from the combined GGR and NSR methods, but with a larger uncertainty estimate to account for method discrepancy and potential spatial variability across the irrigated circle. The resulting emission factor is considered a “maximum” because the measured emissions include naturally occurring background emissions.

Annual N inputs (g N m <sup>-2</sup> )	
Urea applied	18.3 (1.3)
Excreta (dung, urine, effluent)	23.9 (2.5)
Total	42.2 (2.8)
Annual N <sub>2</sub> O emissions (g N m <sup>-2</sup> )	0.51 (0.05)
Maximum emission factor for N <sub>2</sub> O (%)	1.21 (0.15)

than in the footprint of our measurement site. Dividing the N<sub>2</sub>O emissions by the N inputs, the emission factor results as 1.21 (±0.15) %. We consider this as an upper estimate because some fraction of the measured emissions may be natural background emissions. In a chamber experiment in February/March 2014, N<sub>2</sub>O fluxes from the control plots (which were irrigated but received no N) were consistently about 0.5 mg N m<sup>-2</sup> d<sup>-1</sup>, over 35 d, (J. Owens, personal communication, 2015). Integrated over a year, this would amount to 0.18 g N m<sup>-2</sup>. If we tentatively use this value as “background” emissions (even though a fraction of it may still have occurred in response to preceding fertilisations), then the net N<sub>2</sub>O emissions above background would have been 0.33 g N m<sup>-2</sup> and the emission factor 0.78 %. This value is very close to the mean emission factor for dairy cattle excreta, of 0.73 %, from a statistical analysis of 125 field trials in New Zealand (Kelliher et al., 2014). With or without the background included, the observed emission factor is also compatible with the value of 1 % recommended for national greenhouse gas inventories (IPCC, 2006).

At the U UW site, there was no fertiliser applied during the year starting 17 August 2012. There was one winter grazing by 200 cattle in May; Fig. 7 shows a few elevated points in the time series of the N<sub>2</sub>O flux that may have occurred in response to that. There had also been a winter grazing in June 2012, before our recording began. Some of the observed emissions early in the budget year would have originated from the N deposited during that event, possibly amplified by the effects of trampling (Pal et al., 2014). It is therefore likely that the annual emissions at the U UW site, of 0.34 g N m<sup>-2</sup>, were also greater than natural background emissions.

The annual N<sub>2</sub>O emissions at our two sites are comparable to those from grassland sites elsewhere in the world. Phillips et al. (2007) measured N<sub>2</sub>O fluxes from a flood-irrigated, rotationally grazed pasture in south-east Australia. For 2 consecutive years, they obtained annual emissions of 0.55 and 0.44 g N m<sup>-2</sup>, respectively, bracketing the result for the IFR site. Burchill et al. (2014) found, for a rotationally grazed and

intensively fertilised ryegrass pasture in Ireland, annual N<sub>2</sub>O emissions over 4 years to range from 0.44 to 3.44 g N m<sup>-2</sup>. The annual emissions from the IFR site are within this range, near the lower end. Burchill et al. (2014) also measured the annual emissions from ungrazed, unfertilised ryegrass pasture. These ranged from 0.17 to 0.63 g N m<sup>-2</sup>, i.e. from about half to about twice the annual emissions from the U UW site. Soussana et al. (2007) reported annual N<sub>2</sub>O emissions from 10 European grassland sites to range from −0.025 to 0.687 g N m<sup>-2</sup>; management practices and fertiliser application rates at these sites varied considerably. Imer et al. (2013) found annual emissions for three managed ungrazed grassland sites to be from 0.13 to 1.13 g N m<sup>-2</sup>.

#### 4.6 Comparison to other methods

Traditionally, the most common methods to measure trace gas fluxes from or to soils and vegetation have been chamber methods. Their main advantages are high accuracy of the individual sampling, and often low costs (Denmead, 2008). One of their main drawbacks is limited coverage in time (due to operational constraints), though modern autochamber systems with robust field-worthy gas analysers are largely overcoming this disadvantage (van der Weerden et al., 2013; Savage et al., 2014). The other main drawback is that they do not operate at the field scale, which is of particular relevance where gas emissions occur highly concentrated from preferential spots, such as patches of animal excreta. Micrometeorological methods, by contrast, integrate over this spatial variability, and they are in principle continuous in time, except for certain filtering requirements, such as for unsuitable wind direction or insufficient turbulence.

For CH<sub>4</sub> and N<sub>2</sub>O, the most commonly used micrometeorological method presently is eddy covariance, thanks to the advent of a number of fast and precise gas analysers based on laser technologies. Drawbacks of EC are that these analysers are expensive and must be dedicated to a single site, that there are often issues with instrument noise and signal resolution, particularly when fluxes are small for extended periods, and that for periods of small fluxes, the accuracy depends strongly on corrections for density effects and cross-sensitivities (Neftel et al., 2010). Since EC relies on stationary turbulent flow in the surface layer, data from calm nights must be discarded. In this respect, EC is very similar to the GGR method and other variants of flux-gradient methods. Our approach to combine precise mole-fraction measurements of trace gases of interest with EC measurements of CO<sub>2</sub> offers the following advantages over direct EC measurements of the trace gases. First, it allows one to measure at more than one site with the same gas analyser (provided the sites are not too far apart). Second, it allows one to use a multi-gas analyser, such as the FTIR; in fact this is the ideal choice because the mole fractions of the gas of interest and of CO<sub>2</sub> are measured in the same air sample. Third, by then using GGR and NSR as complementary methods to compute

the trace gas fluxes, the sampling includes periods of well-developed and low turbulence and leads to a higher data yield than EC or GGR alone. Of course, the NSR method could potentially also be applied as a complement to direct EC measurements, provided that the EC system includes CO<sub>2</sub>-flux measurements (which is routinely the case) and that these are taken close enough to the ground to keep the footprint of the NSR method representative for the surface of interest (which may be less common).

The GGR method and NSR method each require some optimisation of data filtering criteria: the GGR method for sufficient resolution of CO<sub>2</sub> mole-fraction gradients and positive gas diffusivities, and the NSR method for reliability of nocturnal linear regressions and possibly for suitable wind direction (site-dependent). These criteria appear relatively straightforward, compared to the suite of data quality filters required for the eddy-covariance method. Further, the GGR method and NSR method each employ simple algebraic relationships for gas ratios, which do not require further corrections; in this respect, they are easier to implement than the eddy-covariance method with its rather complex correction procedures involved in the computation of minor trace gas fluxes.

## 5 Conclusions

Continuous year-round measurements of the fluxes of CH<sub>4</sub> and N<sub>2</sub>O at two neighbouring, contrasting pasture sites were obtained with the combination of GGR and NSR methods, both using CO<sub>2</sub> as the reference gas (tracer). The CH<sub>4</sub> and N<sub>2</sub>O fluxes resembled those from other managed grasslands measured with the eddy-covariance or the flux-gradient method. The combination of GGR and NSR methods can thus serve as a viable alternative to eddy covariance and is particularly attractive in paired-site set-ups. However, the NSR method should be applied with caution for trace gases that have strong sources or sinks not co-located with those for the reference gas. Land-use patterns in the surrounding area, as well as regional topography and climate, therefore influence the yield of usable data.

A novelty introduced here, different to the original concept of the NSR method (Kelliher et al., 2002), is the usage of gap-filled CO<sub>2</sub>-flux time series from eddy covariance, instead of CO<sub>2</sub> fluxes from respiration chambers. Mean nocturnal CO<sub>2</sub> fluxes from this approach agreed well with those from chambers, proving its validity.

For N<sub>2</sub>O, the fluxes obtained with the GGR method and NSR method were in reasonable agreement with each other, and they were also fully compatible with the results from a wealth of chamber studies and with recommended emission factors for N<sub>2</sub>O emissions from dairy pasture. The combination of GGR and NSR is thus a reliable option to obtain long-term budgets of the N<sub>2</sub>O exchange of ecosystems on flat land, with the advantage of effective spatial integration

of the source area (which is not guaranteed for chamber systems).

For CH<sub>4</sub>, both the GGR method and the NSR method indicated net emissions from both pasture sites. These were similar to emissions at other grassland sites measured with micrometeorological methods. However, chamber measurements on grassland often show CH<sub>4</sub> fluxes that are 1 or 2 magnitudes smaller and in the opposite direction, indicating CH<sub>4</sub> oxidation in the soil. It is at this stage unclear whether these discrepancies have their origin in the different methods (e.g. the different spatial coverage with chambers and micrometeorological methods) or in different management practices (e.g. fertilisation amounts and frequency, disturbance from animal treading).

**Acknowledgements.** We are grateful to Tony McSeveny and Graeme Rogers for immense technical support in the field, Graham Kettlewell (University of Wollongong) for technical assistance with the FTIR, and the owner of Beacon Farm, Synlait Farms Co. (now renamed to Purata), for supporting our research. We thank Gabriel Moinet for contributing his respiration chamber data to assess nocturnal CO<sub>2</sub> fluxes, and Jennifer Owens for sharing her N<sub>2</sub>O chamber results. This research was undertaken with CRI Core Funding from New Zealand's Ministry of Business, Innovation and Employment.

Edited by: J. Kim

## References

- Acevedo, O. C., Moraes, O. L. L., Degrazia, G. A., Fitzjarrald, D. R., Manzi, A. O., and Campos, J. G.: Is friction velocity the most appropriate scale for correcting nocturnal carbon dioxide fluxes?, *Agr. Forest Meteorol.*, 149, 1–10, 2009.
- AMC (Analytical Methods Committee): Meat and poultry nitrogen factors, *Anal. Methods*, 6, 4493–4495, 2014.
- Balaine, N., Clough, T. J., Beare, M. H., Thomas, S. M., Meenken, E. D., and Ross, J. G.: Changes in relative gas diffusivity explain soil nitrous oxide flux dynamics, *Soil Sci. Soc. Am. J.*, 77, 1496–1505, 2013.
- Baldocchi, D.: Measuring fluxes of trace gases and energy between ecosystems and the atmosphere – the state and future of the eddy covariance method, *Glob. Change Biol.*, 20, 3600–3609, 2014.
- Burchill, W., Li, Dejun, Lanigan, G. J., Williams, M., and Humphreys, J.: Interannual variation in nitrous oxide emissions from perennial ryegrass/white clover grassland used for dairy production, *Glob. Change Biol.*, 20, 3137–3146, 2014.
- DairyNZ: New Zealand Dairy Statistics 2012–2013, DairyNZ and Livestock Improvement Corporation, Hamilton, New Zealand, 52 pp., available at: <http://www.lic.co.nz/user/file/DAIRYSTATISTICS2012-13-WEB.pdf>, (last access: 16 December 2015), 2013.
- Denmead, O. T.: Approaches to measuring fluxes of methane and nitrous oxide between landscapes and the atmosphere, *Plant Soil*, 309, 5–24, 2008.

- Eamus, D., Cleverly, J., Boulain, N., Grant, N., Faux, R., and Villalobos-Vega, R.: Carbon and water fluxes in an arid-zone *Acacia* savanna woodland: An analyses of seasonal patterns and responses to rainfall events, *Agr. Forest Meteorol.*, 182–183, 225–238, doi:10.1016/j.agrformet.2013.04.020, 2013.
- Eugster, W., Zeyer, K., Zeeman, M., Michna, P., Zingg, A., Buchmann, N., and Emmenegger, L.: Methodical study of nitrous oxide eddy covariance measurements using quantum cascade laser spectrometry over a Swiss forest, *Biogeosciences*, 4, 927–939, doi:10.5194/bg-4-927-2007, 2007.
- Felber, R., Munger, A., Neftel, A., and Ammann, C.: Eddy covariance methane flux measurements over a grazed pasture: effect of cows as moving point sources, *Biogeosciences*, 12, 3925–3940, doi:10.5194/bg-12-3925-2015, 2015.
- Griffith, D. W. T., Leuning, R., Denmead, O. T., and Jamie, I. M.: Air-land exchanges of CO<sub>2</sub>, CH<sub>4</sub> and N<sub>2</sub>O measured by FTIR spectrometry and micrometeorological techniques, *Atmos. Environ.*, 36, 1833–1842, 2002.
- Griffith, D. W. T., Deutscher, N. M., Caldow, C., Kettlewell, G., Riggenbach, M., and Hammer, S.: A Fourier transform infrared trace gas and isotope analyser for atmospheric applications, *Atmos. Meas. Tech.*, 5, 2481–2498, doi:10.5194/amt-5-2481-2012, 2012.
- Hortnagl, L. and Wohlfahrt, G.: Methane and nitrous oxide exchange over a managed hay meadow, *Biogeosciences*, 11, 7219–7236, doi:10.5194/bg-11-7219-2014, 2014.
- Hsu, K.-I., Gupta, H. V., Gao, X., Sorooshian, S., and Imam, B.: Self-organizing linear output map (SOLO): An artificial neural network suitable for hydrologic modeling and analysis, *Water Resour. Res.*, 38, 1302, doi:10.1029/2001wr000795, 2002.
- Hunt, J. E., Laubach, J., Barthel, M., Fraser, A., and Phillips, R. L.: Carbon budgets for an irrigated intensively-grazed dairy pasture and an unirrigated winter-grazed pasture, *Biogeosciences Discuss.*, doi:10.5194/bg-2016-46, in review, 2016.
- Imer, D., Merbold, L., Eugster, W., and Buchmann, N.: Temporal and spatial variations of soil CO<sub>2</sub>, CH<sub>4</sub> and N<sub>2</sub>O fluxes at three differently managed grasslands, *Biogeosciences*, 10, 5931–5945, doi:10.5194/bg-10-5931-2013, 2013.
- IPCC: Emissions from livestock and manure management, in: *Guidelines for National Greenhouse Gas Inventories*, Chapter 10, Intergovernmental Panel on Climate Change, 87 pp., [http://www.ipcc-nggip.iges.or.jp/public/2006gl/pdf/4\\_Volume4/V4\\_10\\_Ch10\\_Livestock.pdf](http://www.ipcc-nggip.iges.or.jp/public/2006gl/pdf/4_Volume4/V4_10_Ch10_Livestock.pdf) (last access: 26 February 2015), 2006.
- Kelliher, F. M., Reisinger, A. R., Martin, R. J., Harvey, M. J., Price, S. J., and Sherlock, R. R.: Measuring nitrous oxide emission rate from grazed pasture using Fourier-transform infrared spectroscopy in the nocturnal boundary layer, *Agr. Forest Meteorol.*, 111, 29–38, 2002.
- Kelliher, F. M., Cox, N., van der Weerden, T. J., de Klein, C. A. M., Luo, J., Cameron, K. C., Di, H. J., Giltrap, D., and Rys, G.: Statistical analysis of nitrous oxide emission factors from pastoral agriculture field trials conducted in New Zealand, *Environ. Pollut.*, 186, 63–66, 2014.
- Kormann, R. and Meixner, F. X.: An analytical footprint model for non-neutral stratification, *Bound.-Lay. Meteorol.*, 99, 207–224, 2001.
- Kroon, P. S., Hensen, A., Jonker, H. J. J., Zahniser, M. S., van 't Veen, W. H., and Vermeulen, A. T.: Suitability of quantum cascade laser spectroscopy for CH<sub>4</sub> and N<sub>2</sub>O eddy covariance flux measurements, *Biogeosciences*, 4, 715–728, doi:10.5194/bg-4-715-2007, 2007.
- Kroon, P. S., Hensen, A., Jonker, H. J. J., Ouwersloot, H. G., Vermeulen, A. T., and Bosveld, F. C.: Uncertainties in eddy covariance flux measurements assessed from CH<sub>4</sub> and N<sub>2</sub>O observations, *Agr. Forest Meteorol.*, 150, 806–816, 2010.
- Laubach, J., Kelliher, F. M., Knight, T., Clark, H., Molano, G., and Cavanagh, A.: Methane emissions from beef cattle – a comparison of paddock- and animal-scale measurements, *Aust. J. Exp. Agric.*, 48, 132–137, 2008.
- Laubach, J., Bai, Mei, Pinares-Patino, C. S., Phillips, F. A., Naylor, T. A., Molano, G., Cardenas Rocha, E. A., and Griffith, D. W. T.: Accuracy of micrometeorological techniques for detecting a change in methane emissions from a herd of cattle, *Agr. Forest Meteorol.*, 176, 50–63, 2013.
- Leahy, P., Kiely, G., and Scanlon, T. M.: Managed grasslands: A greenhouse gas sink or source?, *Geophys. Res. Lett.*, 31, L20507, doi:10.1029/2004GL021161, 2004.
- Li, Z. and Kelliher, F. M.: Methane oxidation in freely and poorly drained grassland soils and effects of cattle urine application, *J. Environ. Qual.*, 36, 1241–1248, 2007.
- McMillan, A. M. S., Goulden, M. L., and Tyler, S. C.: Stoichiometry of CH<sub>4</sub> and CO<sub>2</sub> flux in a California rice paddy, *J. Geophys. Res.*, 112, G01008, doi:10.1029/2006JG000198, 2007.
- Merbold, L., Eugster, W., Stieger, J., Zahniser, M., Nelson, D., and Buchmann, N.: Greenhouse gas budget (CO<sub>2</sub>, CH<sub>4</sub> and N<sub>2</sub>O) of intensively managed grassland following restoration, *Glob. Change Biol.*, 20, 1913–1928, 2014.
- MfE: New Zealand's Greenhouse Gas Inventory 1990–2013, Ministry for the Environment, Wellington, New Zealand, 450 pp., <http://www.mfe.govt.nz/publications/climate-change/new-zealands-greenhouse-gas-inventory-1990-2013>, last access: 23 June 2015.
- Mills, A. and Moot, D. J.: Annual dry matter, metabolisable energy and nitrogen yields of six dryland pastures six and seven years after establishment, *Proceedings of the New Zealand Grassland Association*, 72, 177–184, 2010.
- Miyata, A., Leuning, R., Denmead, O. T., Kim, Joon, and Harazono, Y.: Carbon dioxide and methane fluxes from an intermittently flooded paddy field, *Agr. Forest Meteorol.*, 102, 287–303, 2000.
- Moncrieff, J. B., Malhi, Y., and Leuning, R.: The propagation of errors in long-term measurements of land-atmosphere fluxes of carbon and water, *Glob. Change Biol.*, 2, 231–240, 1996.
- Montzka, S. A., Dlugokencky, E. J., and Butler, J. H.: Non-CO<sub>2</sub> greenhouse gases and climate change, *Nature*, 476, 43–50, doi:10.1038/nature10322, 2011.
- Mudge, P. L., Wallace, D. F., Rutledge, S., Campbell, D. I., Schipper, L. A., and Hosking, C. L.: Carbon balance of an intensively grazed temperate pasture in two climatically contrasting years, *Agric. Ecosyst. Environ.*, 144, 271–280, 2011.
- Neftel, A., Spirig, C., and Ammann, C.: Application and test of a simple tool for operational footprint evaluations, *Environ. Pollut.*, 152, 644–652, 2008.
- Neftel, A., Ammann, C., Fischer, C., Spirig, C., Conen, F., Emmenegger, L., Tuzson, B., and Wahlen, S.: N<sub>2</sub>O exchange over managed grassland: Application of a quantum cascade laser spectrometer for micrometeorological flux measurements, *Agr. Forest Meteorol.*, 150, 775–785, 2010.

- Nicolini, G., Castaldi, S., Fratini, G., and Valentini, R.: A literature overview of micrometeorological CH<sub>4</sub> and N<sub>2</sub>O flux measurements in terrestrial ecosystems, *Atmos. Environ.*, 81, 311–319, 2013.
- Nieveen, J. P., Campbell, D. I., Schipper, L. A., and Blair, I. J.: Carbon exchange of grazed pasture on a drained peat soil, *Glob. Change Biol.*, 11, 607–618, 2005.
- Oke, T. R.: *Boundary Layer Climates*, 2nd ed., Methuen Press, London, 435 pp., 1987.
- Pal, P., Clough, T. J., and Kelliher, F. M.: Sources of N<sub>2</sub>O-N following simulated animal treading of ungrazed pastures, *J. Agric. Res.*, 57, 202–215, 2014.
- Pendall, E., Schwendenmann, L., Rahn, T., Miller, J. B., Tans, P. P., and White, J. W. C.: Land use and season affect fluxes of CO<sub>2</sub>, CH<sub>4</sub>, CO, N<sub>2</sub>O, H<sub>2</sub> and isotopic source signatures in Panama: evidence from nocturnal boundary layer profiles, *Glob. Change Biol.*, 16, 2721–2736, 2010.
- Phillips, F. A., Leuning, R., Baigent, R., Kelly, K. B., and Denmead, O. T.: Nitrous oxide flux measurements from an intensively managed irrigated pasture using micrometeorological techniques, *Agr. Forest Meteorol.*, 143, 92–105, 2007.
- Price, S. J., Kelliher, F. M., Sherlock, R. R., Tate, K. R., and Condron, L. M.: Environmental and chemical factors regulating methane oxidation in a New Zealand forest soil, *Aust. J. Soil Res.*, 42, 767–776, 2004.
- Savage, K., Phillips, R., and Davidson, E.: High temporal frequency measurements of greenhouse gas emissions from soils, *Biogeosciences*, 11, 2709–2720, doi:10.5194/bg-11-2709-2014, 2014.
- Schaufli, G., Kitzler, B., Schindlbacher, A., Skiba, U., Sutton, M. A., and Zechmeister-Boltenstern, S.: Greenhouse gas emissions from European soils under different land use: effects of soil moisture and temperature, *Eur. J. Soil Sci.*, 61, 683–696, 2010.
- Schmid, H. P.: Source Areas for Scalars and Scalar Fluxes, *Bound.-Lay. Meteorol.*, 67, 293–318, 1994.
- Schrier-Uijl, A. P., Kroon, P. S., Hendriks, D. M. D., Hensen, A., Van Huissteden, J., Berendse, F., and Veenendaal, E. M.: Agricultural peatlands: towards a greenhouse gas sink – a synthesis of a Dutch landscape study, *Biogeosciences*, 11, 4559–4576, doi:10.5194/bg-11-4559-2014, 2014.
- Smith, K. A., Ball, T., Conen, F., Dobbie, K. E., Massheder, J., and Rey, A.: Exchange of greenhouse gases between soil and atmosphere: interactions of soil physical factors and biological processes, *Eur. J. Soil Sci.*, 54, 779–791, 2003.
- Soussana, J. F., Allard, V., Pilegaard, K., Ambus, P., Amman, C., Campbell, C., Ceschia, E., Clifton-Brown, J., Czobel, S., Domingues, R., Flechard, C., Fuhrer, J., Hensen, A., Horvath, L., Jones, M., Kasper, G., Martin, C., Nagy, Z., Neftel, A., Raschi, A., Baronti, S., Rees, R. M., Skiba, U., Stefani, P., Manca, G., Sutton, M., Tuba, Z., and Valentini, R.: Full accounting of the greenhouse gas (CO<sub>2</sub>, N<sub>2</sub>O, CH<sub>4</sub>) budget of nine European grassland sites, *Agric. Ecosyst. Environ.*, 121, 121–134, 2007.
- Tuzson, B., Hiller, R. V., Zeyer, K., Eugster, W., Neftel, A., Ammann, C., and Emmenegger, L.: Field intercomparison of two optical analyzers for CH<sub>4</sub> eddy covariance flux measurements, *Atmos. Meas. Tech.*, 3, 1519–1531, doi:10.5194/amt-3-1519-2010, 2010.
- Van der Weerden, T. J., Clough, T. J., and Styles, T. M.: Using near-continuous measurements of N<sub>2</sub>O emission from urine-affected soil to guide manual gas sampling regimes, *J. Agric. Res.*, 56, 60–76, 2013.
- Wilson, J. D.: Turbulent Schmidt numbers above a wheat crop, *Bound.-Lay. Meteorol.*, 148, 255–268, 2013.
- Woodward, S. L., Waghorn, G. C., Bryant, M. A., and Mandok, K.: Are high breeding worth index cows more feed conversion efficient and nitrogen use efficient?, *Proceedings of the New Zealand Society of Animal Production*, 71, 109–113, 2011.